Polymerization-Induced Self-Assembly of Poly(ethylene glycol)-*block*-Poly(*N*-vinylcaprolactam)

Satu Häkkinen

Master's Thesis

University of Helsinki
Department of Chemistry

10/2017

HELSINGIN YLIOPISTO
HELSINGFORS UNIVERSITET
UNIVERSITY OF HELSINKI
MATEMAATTIS-LUONNONTIETEELLINEN TIEDEKUNTA
MATEMATISK-NATURVETENSKAPLIGA FAKULTETEN
FACULTY OF SCIENCE

Tiedekunta – Fakultet – Faculty	Koulutusohjelma – Utbildningsprogram – Degree programme
Faculty of Science	Degree Programme in Chemistry

Tekijä – Författare – Author
Satu Häkkinen

Työn nimi – Arbetets titel – Title
Polymerization-Induced Self-Assembly of Poly(ethylene glycol)-*block*-Poly(*N*-vinylcaprolactam)

Työn laji – Arbetets art – Level	Aika – Datum – Month and year	Sivumäärä – Sidoantal – Number of pages
Master's Thesis	10/2017	52

Tiivistelmä – Referat – Abstract

Preparation of polymer nanoparticles has become of great interest to polymer scientists due to their wide range of applications. Block copolymer nano-objects have been studied for decades, however new production methods are still needed to achieve better commercial viability and thus a wider use of the materials. Polymerization-induced self-assembly (PISA) is a new approach to preparing block copolymer nanoparticles, in which the polymerization of the second block and the self-assembly of the particles are achieved in one step. The method exploits the growing insolubility of the propagating chain to induce the self-assembly already during the polymerization, yielding nano-objects of various morphologies. The approach has gained significant attention in the last few years, and its popularity is expected to grow in the future.

This thesis presents the fundamentals of PISA, while offering insight into both the benefits and challenges of the method. The focus of the work is on aqueous emulsion RAFT PISA formulations. Additionally, a new method for the preparation of poly(ethylene glycol)-*block*-poly(*N*-vinylcaprolactam) nanoparticles through PISA was developed. The synthesis exploited the lower critical solution temperature behaviour of poly(*N*-vinylcaprolactam) by conducting the polymerization of said block above its phase transition temperature in water. The polymerizations were carried out as RAFT reactions in emulsion and the resulting particles were characterized by dynamic light scattering. The method yielded particles of 200 nm in diameter that dissolved in water upon cooling to room temperature. Moreover, the purified and dried polymers were analysed using size-exclusion chromatography, NMR spectroscopy and turbidimetry. Preliminary tests showed that the stable particles can be physically crosslinked with salicylic acid to prevent dissolution upon cooling.

Avainsanat – Nyckelord – Keywords
Polymerization-induced self-assembly, RAFT, emulsion polymerization, poly(*N*-vinylcaprolactam)

Säilytyspaikka – Förvaringställe – Where deposited
Kumpula Campus Library

Muita tietoja – Övriga uppgifter – Additional information

Table of contents

Abbreviations and Symbols

ACN	acetonitrile
CTA	chain transfer agent
$Đ_M$	dispersity
DLS	dynamic light scattering
DMF	*N*,*N*-dimethylformamide
HEPES	2-[4-(2-hydroxyethyl)piperazin-1-yl]ethanesulfonic acid
LCST	lower critical solution temperature
M_n	number average molecular weight
MADIX	macromolecular design by interchange of xanthates
mCTA	macro-chain transfer agent
mPEG	poly(ethylene glycol) methyl ether
NMR	nuclear magnetic resonance
NVCL	*N*-vinylcaprolactam
PEG	poly(ethylene glycol)
PEO	poly(ethylene oxide)
PISA	polymerization-induced self-assembly
PNVCL	poly(*N*-vinylcaprolactam)
R_h	hydrodynamic radius
RAFT	reversible addition-fragmentation chain transfer
SEC	size-exclusion chromatography
T_c	cloud point temperature
TBAB	tetrabutylammonium bromide
Tris	2-amino-2-(hydroxymethyl)propane-1,3-diol

Introduction

Polymer nanoparticles are colloidal materials of 10-1000 nm in diameter. They can be prepared by various polymerization and post-polymerization processing routes.[1] The materials have been found useful in a wide array of modern technologies, including electronics, medicine, and environmental applications. As the particles are typically designed to suit a specific application, the production is often set with limitations as to which preparation methods can be used. The preparation is rather straightforward when the particles can be produced using emulsion polymerization. However, multiple steps are often required, as is the case when the polymer must be prepared prior to the particle formation step. Such routes can result in time-consuming procedures that are not cost-effective. Additionally, the fundamental knowledge regarding the preparation of polymer nanoparticles is still limited.[1] These factors indicate a need for new efficient and precise techniques that can be used to produce particles with controlled sizes and morphologies.

Polymerization-induced self-assembly (PISA) is a novel technique for producing block copolymer nanoparticles in one step. While being a newly developed approach to an old area of interest in polymer research, it has already been shown to offer significant advantages over conventional emulsion polymerization and self-assembly methods.[2] The technique produces block copolymer nano-objects of various sizes and shapes via living polymerization techniques. The genius of the PISA approach lies in the variety of morphologies that can be achieved with relatively little effort. These morphologies can offer advantages over the classical spherical micelle, such as higher loading capacities or the ability to encapsulate both hydrophobic and hydrophilic materials in one particle.[3] Moreover, the versatility of PISA is illustrated by the various monomers and solvents that have already been used in the reactions.[2] The reactions often exhibit high conversions and reaction rates at high concentrations, while maintaining a low viscosity. Such systems are particularly promising for industrial-scale production.

The growing popularity of the PISA concept is demonstrated by **Figure 1**. Despite being a new area of research, it has already contributed to materials science as a convenient route to sterilizable hydrogels[4], engine oil additives[5], intracellular delivery vehicles[6], Pickering emulsifiers[7], and other materials of interest. The number of publications presenting new PISA formulations can be expected to grow fast in the near future. A likely new trend is to use the stimulus-responsiveness of the material, such as its lower critical solution temperature, for triggering the self-assembly during polymerization.[8]

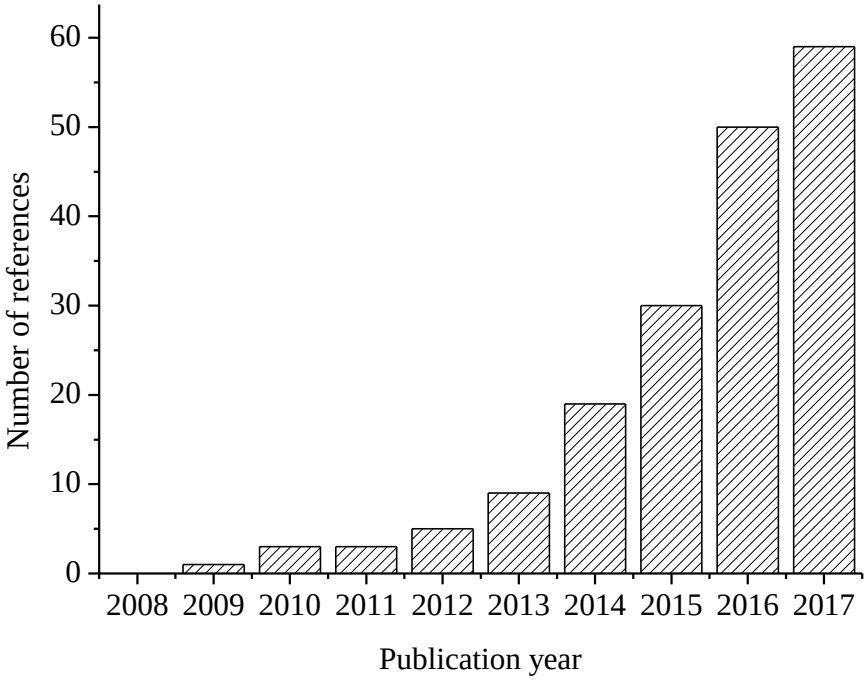

Figure 1 Number of PISA publications per year. SciFinder search for "polymerization-induced self-assembly" as entered and without duplicates, years 2008-2017 (04.10.2017).

This thesis provides an overview of the recently developed PISA approach for producing block copolymer nanoparticles. The primary focus will be on aqueous emulsion PISA syntheses. Furthermore, a new PISA formulation will be presented. All concepts relevant to the experimental work will be first introduced in the literature part of the thesis. First, the concept of PISA is discussed in more depth. Secondly, the properties of *N*-vinylcaprolactam will be reviewed to illuminate the choice of monomer in the experimental work. The chapter will be followed by the principles of reversible addition-fragmentation chain transfer polymerization, and its relevance in block copolymer synthesis and emulsion systems. Finally, emulsion polymerization and the origins of PISA systems will be discussed, along with some challenges faced in PISA syntheses.

I. LITERATURE PART

1. Polymerization-Induced Self-Assembly

Block copolymer self-assembly has been studied since the early 1960s.[9] The focus of the research has slowly shifted from bulk processes, which are now well understood, to self-assembly in solution, introducing an additional level of complexity to the system. The popularity of self-assembling copolymers lies in the wide variety of suitable monomers and potential applications. The resulting structures can be used for loading and releasing of small molecules[10], controlled exposure of hidden, covalently bound units[11], preparation of metal nanoparticles[12], and surface modification purposes.[13] Polymer aggregates exhibit superior mechanical and physical properties[9] and low critical micelle concentrations[13] when compared to their small-molecule counterparts.

The most popular conventional approach for achieving the self-assembly of a block polymer is a two-step process.[9] The copolymer is initially added in a common solvent, in which both blocks are readily soluble. The solvency is then reduced for one of the blocks by adding a selective solvent to induce microphase separation. The addition is continued until the content of the selective solvent is much higher than the required amount for the aggregation to take place. Finally, an excess of solvent is added to lock the resulting morphologies. In many cases the common solvent can be removed by dialysis against the selective solvent. Other methods for producing aggregates in a controlled fashion include electroformation[14] and microfluidic techniques[15], amongst others.[9] The approaches have been shown to yield a variety of morphologies, such as spherical micelles[16], worms[17], vesicles[18], and lamellae[19]. Some systems have reported to undergo a transformation of the structure under suitable conditions.[18] The resulting morphology is determined by the degree of stretching of the core-forming blocks, the interfacial tension between the core and the solvent, and the repulsive interactions between the chains forming the outer layer.[9] Generally, the final copolymer concentrations achieved by these routes are too low for commercial production.[2] Finding new, more convenient methods remains a goal for polymer scientists.

A more recent approach to copolymer self-assembly exploits the growing insolubility of a propagating polymer chain to induce the self-assembly already during the polymerization process. The strategy typically utilizes a soluble homopolymer block that is extended by the addition of another monomer (**Scheme 1**).[2] As more monomer is added, the growing block

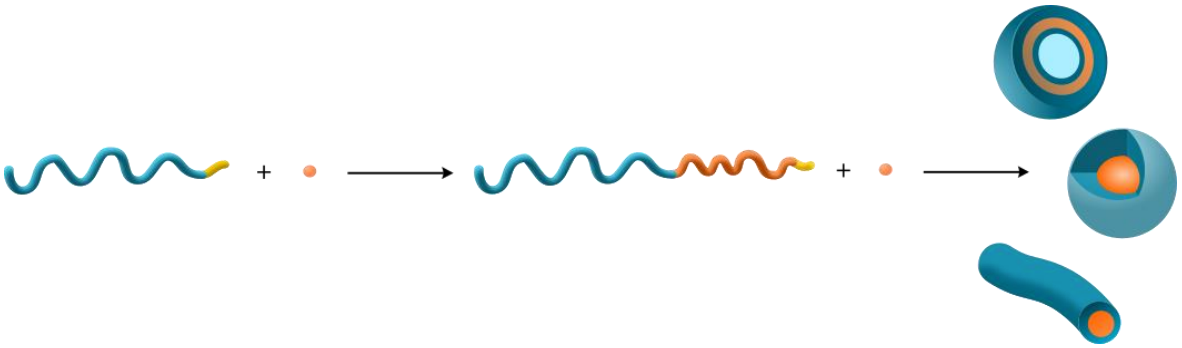

Scheme 1 Schematic representation of a RAFT-mediated PISA reaction. A macro-chain transfer agent is extended with monomer. The growing chain will eventually become insoluble in the reaction medium and result in the self-assembly of the chain, yielding particles such as vesicles, spheres or worms.

gradually becomes insoluble, and the polymer self-assembles to compensate for the unfavorable solvent interactions. This new route to creating block copolymer nano-objects is known as polymerization-induced self-assembly (PISA). It is most often conducted by using reversible addition-fragmentation chain transfer (RAFT) polymerization, however other living polymerizations, such as nitroxide mediated[20] and atom transfer radical polymerizations[21], have been used as well. Successful reactions have been carried out in emulsion and dispersion in polar and non-polar media, resulting in even more unusual morphologies, such as yolk/shell particles[22], jellyfish[23], and framboidal vesicles.[2] The particle morphology is dictated by the copolymer concentration and the block copolymer composition. The approach allows fast preparation of polymer colloids at high concentrations, often resulting in low dispersity products. The versatility of PISA is further illustrated in the excellent review of Canning *et al.*[2]

1.1. PISA of Stimuli-Responsive Polymers

Stimuli-responsive polymers have not been left out from PISA research. Multiple studies have been published where PISA was used to prepare thermoresponsive particles. Blanazs *et al.* reported the synthesis of poly(glycerol monomethacrylate)-*block*-poly(2-hydroxypropyl methacrylate) hydrogels that underwent worm-to-sphere transition upon cooling.[4] The transition gave rise to thermoreversible degelation of the free-standing gel, yielding a free-flowing solution. The thermoreversibility allowed facile sterilization of the material using ultrafiltration, and the method could thus offer a convenient route to producing sterilizable gels for cell cultures. Conversely, Fielding *et al.* published the preparation of thermoresponsive poly(lauryl methacrylate)-*block*-poly(benzyl methacrylate)

worm gels that underwent worm-to-sphere transition upon heating.[24] Reports can also be found on the use of pH-responsive polymers. Lovett *et al.* used a poly(glycerol monomethacrylate)-based macro-chain transfer agent (mCTA) to polymerize 2-hydroxypropyl methacrylate.[25] Reaction at pH 3.5 resulted in the formation of copolymer worms that underwent worm-to-sphere transition upon addition of base. The pH-responsive behavior was achieved through the incorporation of a single, terminal carboxylic acid group in each mCTA chain. Thus, only a minimal amount of base was required to induce the reversible transition. A more unusual stimulus was used by Zetterlund *et al.* in the preparation of poly(4-vinylpyridine)-*block*-polystyrene.[26] The group reported the synthesis of copolymers with various morphologies. The presence of gaseous CO_2 was shown to promote the formation of copolymer rods instead of vesicles at high degrees of polymerization.

A very recent take on PISA considers the possibility to use thermally-triggered aggregation to yield self-assembled particles. The first paper to present the concept, specifically referred to as polymerization-induced thermal self-assembly (PITSA), was published by Figg *et al.* in 2015.[8] The group polymerized *N*-isopropylacrylamide in the presence of a hydrophilic RAFT agent consisting of *N*,*N*-dimethylacrylamide and acrylic acid units. By carrying out the reaction above the phase-transition temperature of the growing poly(*N*-isopropylacrylamide) block, the polymer underwent self-assembly yielding spherical, worm-like and vesicular particles. The work lays the foundation for a completely new type of PISA formulations. The wide range of stimuli-responsive polymers offers new opportunities for research on self-assembling systems. Potential options for the growing block include numerous other lower critical solution temperature (LCST) polymers[27], such as poly(*N*-vinylcaprolactam) and poly[(*N*,*N*-dimethylamino)ethyl methacrylate]. In contrast, upper critical solution temperature behavior can be utilized by introducing a block for which the solubility in water decreases upon cooling.[28] Such thermally-induced self-assemblies exhibit limited operating temperature ranges, unless stabilized appropriately. Possible ways to achieve this include physical crosslinking through hydrogen bonding[10] or ionic interactions, and chemical crosslinking by addition of a bifunctional monomer[29] or by post-polymerization modification.[30]

2. Poly(*N*-vinylcaprolactam)

Poly(*N*-vinylcaprolactam) (PNVCL, **Scheme 2**) is the second-most used temperature-responsive polymer.[31] It is widely utilized in environmental, catalytic, biomedical, and bioanalytical applications in various forms of copolymers, hydrogels, and polymer architectures. The first publications on the polymerization of *N*-vinylcaprolactam date back to 1952[32] and 1968[33]. Despite the long history of research, the popularity of PNVCL still suffers from difficulties encountered in the production of the polymer. Reactions in bulk and in solution have been reported to result in high molecular weights, high dispersities and even in bimodal distributions of the product.[34] The propagation rate of the monomer is relatively high due to lack of conjugation and thus an absence of resonance stabilization in the structure. The use of chain transfer agents (CTAs) has helped researchers overcome some of the problems. RAFT reactions, particularly those utilizing xanthates as the CTA, have been reported to yield dispersities as low as 1.1 for products ranging from 18,000 to 150,000 g mol^{-1}.[35] Successful reactions have also been carried out using cobalt mediated radical polymerization.[31]

PNVCL is soluble in polar and non-polar media, and has been polymerized in a variety of solvents, such as toluene[33], 1,4-dioxane[36], and *N*,*N*-dimethylformamide (DMF)[37], using free radical polymerization methods. The water solubility of the monomer is low, approximately 4 g l^{-1}. However, due to the low melting point of 35-38 ^{o}C, the polymer can be synthesized in aqueous media using emulsion processes.[38] Unlike the monomer, the resulting polymer is readily soluble in water. One of the key properties of PNVCL is its LCST behavior in water, meaning that the polymer undergoes coil-to-globule transition at its phase transition temperature upon heating (**Scheme 3**). PNVCL belongs to Type I LCST polymers, which represent the classical Flory-Huggins behavior.[39] For such materials, the position of the critical composition shifts towards lower concentration with increasing molar mass. The

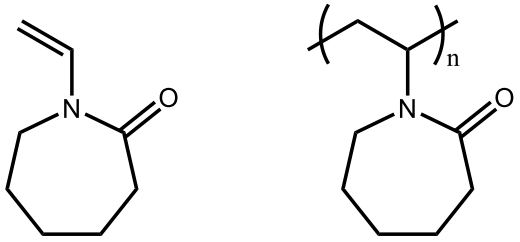

Scheme 2 Molecular structures of *N*-vinylcaprolactam (left) and poly(*N*-vinylcaprolactam) (right).

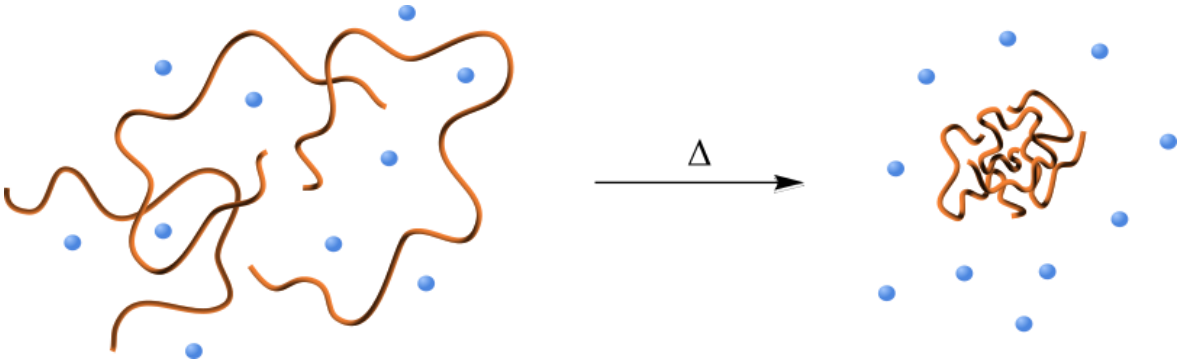

Scheme 3 Schematic representation of the LCST behavior of PNVCL. Upon heating above the critical temperature, the polymer chains become insoluble and collapse, forming aggregates.

cloud point temperature of PNVCL can typically be found between 30-40 ºC [31], that is, in the temperature range relevant to many biological systems. The transition temperature can be increased or decreased by the incorporation of a second monomer.[40] Moreover, copolymerization allows for the incorporation of hydrophilic, hydrophobic and ionic repeating units in the polymer, widening the range of PNVCL-based materials. Numerous reports on the design of various architectures, such as graft copolymers, hyperbranched and protein-like structures, and core-shell gels, can be found in literature.[31] The instability of the propagating *N*-vinylcaprolactam (NVCL) radical can pose a problem when copolymerized with monomers such as methacrylates that form relatively stable radicals.[41] Such conditions can result in low reactivity and thus low NVCL content in the product. The use of controlled radical polymerization techniques for synthesizing PNVCL led to the development of various PNVCL-based block copolymers. Liang *et al.* reported the preparation of a series of block copolymers of PNVCL and poly(*N*-vinyl-2-pyrrolidone) using RAFT.[42] The phase transition temperature of the product could be fine-tuned by controlling the length of the second block. The dispersities of the products varied between 1.4-1.7. Liu *et al.* reported the polymerization of NVCL in DMF using a xanthate-terminated poly(ethylene glycol) (PEG) mCTA.[43] The dispersities of the products with molecular weights of 7,700-41,200 g mol^{-1} ranged from 1.0-1.1, indicating an exceptionally good control over the reaction.

One of the biggest selling points of PNVCL has been its biocompatibility. The polymer has already been used in cosmetics and various biomedical materials. The biocompatibility of synthetic polymers can often be enhanced by adding steric repulsion against protein absorption.[44] This can be achieved by grafting the polymer with materials such as poly(ethylene oxide) (PEO) – a hydrophilic polymer widely used in medical and biological

applications. The first study on the cytotoxicity of PNVCL and PNVCL-*graft*-PEO was published by Vihola *et al*. in 2005.[45] Research has since been done on the cytotoxicity of PNVC-grafted chitosan[46], folate-conjugated PNVCL-*b*-PEG micelles[47], PNVCL-based microgels[48,49], PVCL-based micro- and nanoparticles[50,51], and poly(*N*-vinylcaprolactam)-*block*-poly(*N*-vinylpyrrolidone)[42]. All studies indicated good tolerance of the cells towards the tested materials. The biocompatibility and convenient LCST make PNVCL an attractive option for pharmaceutical applications. Markvicheva *et al.* studied entrapment of cells in PNVCL particles by exploiting the phase transition behavior of the polymer already in 1991.[52] The hydrogel was stabilized by ovalbumin at 40 ºC, and formed granules upon stirring. Vihola *et al.* expanded on the idea of particle stabilization by preparing drug-loaded, physically crosslinked PNVCL hydrogel particles.[10] Concentrated polymer solution containing drug molecules was added dropwise to aqueous salicylic acid. At 37 ºC, the polymer droplets solidified yielding drug-loaded hydrogel particles. The thermosensitive particles were stabilized by the physical crosslinker and showed no flocculation.

3. RAFT Polymerization

Reversible addition-fragmentation chain transfer polymerization is a type of controlled radical polymerization that makes use of a thiocarbonylthio CTA. Developed in 1998 by the Commonwealth Scientific and Industrial Research Organisation group in Australia[53], it is the most recent of the controlled free radical methods, and has had a great impact on the development of free radical polymerization. RAFT has been reported to be the most versatile of all the living radical polymerization techniques in terms of reaction conditions, compatible monomers, its tolerance to functionalities and the variety of complex macromolecular architectures that can be created.[54] The use of multifunctional RAFT agents allows the production of star, brush and comb polymers. In its simplest form, RAFT polymerization can be carried out by introducing a suitable CTA in a conventional free-radical polymerization system. Unlike in conventional reactions, predictable molecular weights and low dispersities can be achieved while keeping the end groups active for further reaction.

3.1. Mechanism of the RAFT Process

The mechanism of RAFT polymerization is presented in **Scheme 4**. The chain radical is produced using a conventional initiator. In the pre-equilibrium stage of the reaction, a

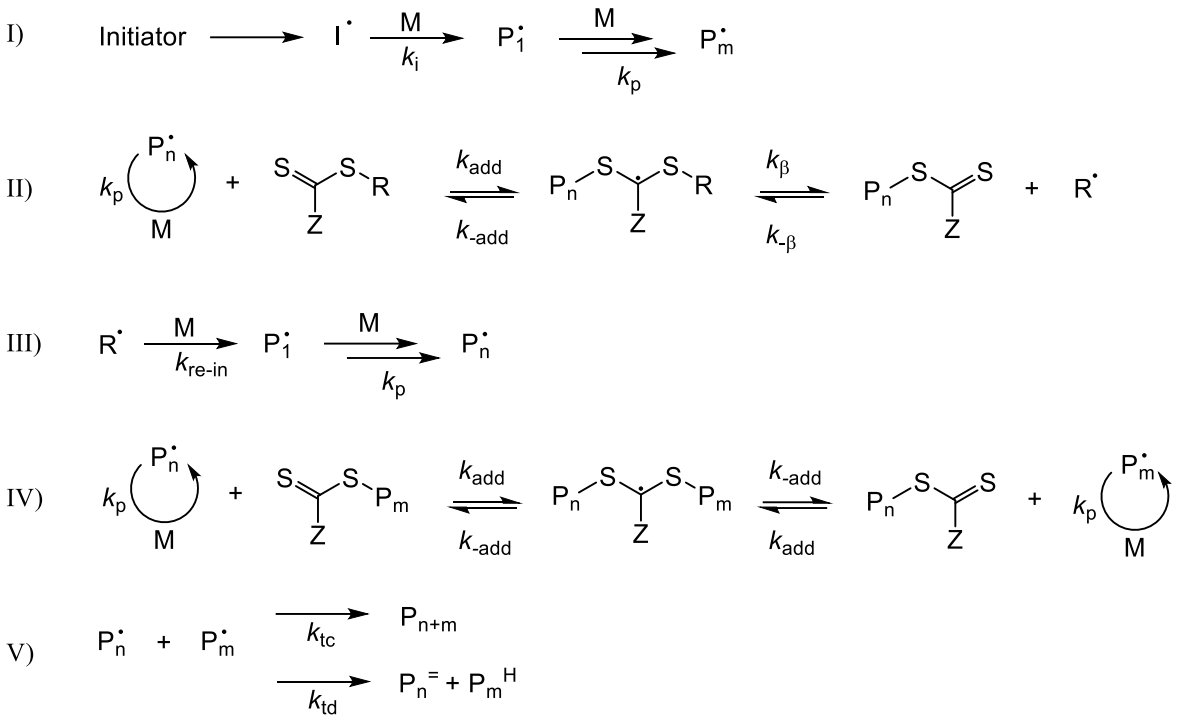

Scheme 4 Simplified mechanism of RAFT polymerization.[55,56] Initiation (I), pre-equilibrium (II), reinitiation (III), main equilibrium (IV) and termination reactions (V) are shown.

propagating chain radical will undergo addition to the CTA, forming an intermediate radical. The intermediate will then fragment reversibly, preferably resulting in a dormant polymeric chain and a new radical. A fragmented R group will reinitiate polymerization. In the main equilibrium phase, the addition of a chain radical induces the fragmentation of another chain. The number of dormant molecules in the reaction mixture equals the number of CTA molecules added. Due to chain equilibration, the amount of termination and unwanted chain transfer reactions is kept low.

The livingness of RAFT polymerization requires careful consideration of the following factors.[55] First, the CTA must be consumed very early in the reaction by a fast addition of the chain radical, resulting in the fragmentation of the reinitiating radical. The reinitiation step must be at least as fast as propagation. Secondly, the rate constant of the chain radical addition and fragmentation in the main equilibrium must be much faster than propagation. This requirement is the key to producing polymers with low dispersities, as a fast rate constant of exchange ensures that chains of equal length are obtained. Finally, the intermediate radical must not be susceptible to side reactions. The selection of Z and R groups has a great impact on the properties of the RAFT agent. The Z group strongly affects

the stability of the radical intermediate.[54] It can also activate or deactivate the thiocarbonyl double bond. On the other hand, the R group determines the rate of forward fragmentation of the intermediate radical. It should also readily reinitiate the addition of further monomer. Parameters to consider include resonance stabilization, electron-withdrawing ability, and steric bulk of the R group.

3.2. MADIX

The macromolecular design by interchange of xanthates (MADIX) process was discovered perhaps concurrently with RAFT polymerization by a different research group. When the first pieces of CTA research were published in 1986[56], ultimately leading to the development of RAFT, another group of researchers were working on the radical chemistry of xanthates. The work published by Zard *et al.* in 1988 presented the use of degenerative transfer of radicals to xanthates in order to facilitate the addition of the radicals to double bonds.[57] The new approach diminished radical quenching through competitive reactions. It was first applied to organic synthesis and eventually reached a wider audience.

From a mechanistical point of view, RAFT and MADIX processes are identical. The difference of the concepts lies in the CTA. RAFT agents have the general structure Z—C(=S)S—R, whereas MADIX refers to xanthates only, *i.e.* Z = OZ′ (**Scheme 5**). The double bond character of the C=S bond is decreased in xanthates due to conjugation with nonbonded electrons on the adjacent oxygen.[58] Such structure results in delocalization of the π electrons and consequently in a lowered rate of addition of a chain radical at sulfur. Thus, the Z group strongly affects the overall rate of chain transfer. Alkyl xanthates have been deemed unsuitable RAFT agents for strongly reactive monomers, but may be suitable for the polymerization of weakly reactive ones.[55] Delocalization can be reduced by an electron-withdrawing substituent bonded to the oxygen atom. By the addition of a group such as carbonyl or phenyl, thiocarbonylthio compounds can be tailored suitable for strongly reactive monomers as well.

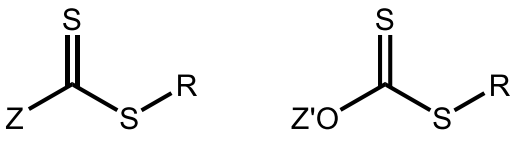

Scheme 5 Molecular structures of thiocarbonylthio compounds (left) and xanthates (right).

Generally speaking, the controlled free radical polymerization of unconjugated monomers has proved challenging.[59] MADIX polymerization has been shown to resolve some of the problems encountered in the polymerization of NVCL, such as high dispersities of the products.[35,60] Nieuwenhove *et al.* demonstrated the successful MADIX polymerization of NVCL in water-ethanol mixtures.[61] The dispersities varied between 1.14 and 1.39, while the molar masses ranged from 9,000 to 12,000 g mol^{-1}.

3.3. Block Copolymer Synthesis

Given the potential of RAFT in macromolecular engineering[59], block copolymers are among the simplest possible polymeric architectures. Two approaches to block copolymer synthesis via RAFT exist. The choice of approach is dependent on the compatibility of all monomers with the RAFT method. The first route is sequential monomer addition, in which one monomer is polymerized quantitatively before the addition of a second monomer. The initial homopolymer may either be purified between the reactions, or the second monomer can be added directly to the system. If the latter is preferred, the addition is generally done below 90% conversion of the first monomer to ensure that the chain-end functionality of the first block is maintained.[54] The product will exhibit a monomer gradient between the homopolymer blocks, as the addition of the first monomer will compete with the addition of the second monomer until all of the former has been consumed. To obtain a low dispersity product and to ensure the attachment of the blocks, the fragmentation ability of the first block must be equal or greater than that of the second block. This will allow propagation of all the initial homopolymer chains in the second step. The resulting product will always have homopolymer contamination, as new chains are created from initiating radicals in the second step. The method is suitable not only for AB diblock copolymers, but also for the production of type ABA triblock copolymers. Triblock products can be obtained by using CTAs with difunctional R groups[62] or symmetrical trithiocarbonates containing two reinitiating R groups[63].

The second approach involves the end-group modification of a homopolymer, resulting in a mCTA. The mCTA can then be used in the polymerization of a subsequent monomer to yield a block copolymer. Modification of functionalities at both chain ends allows the chain to grow at both ends in the subsequent reaction, yielding a triblock product. The most prominent advantage of this route is the possibility to utilize polymers produced by other polymerization mechanisms. Numerous studies have been published using this approach. Amongst other materials, the method has gained popularity in the synthesis of PEG-based

block copolymers. Hong *et al.* prepared diblock and triblock copolymers using dithiobenzoyl-terminated PEGs to control the polymerization of *N*-isopropylacrylamide in THF.[64] The products exhibited dispersities of 1.2 and lower. Shi *et al.* used xanthate-modified PEGs to carry out MADIX polymerization of *N*-vinylformamide in DMSO.[65] However, the dispersities of the resultant block copolymers were high, ranging from 1.7 to 2.3, possibly due to chain transfer side reactions.

Polymers prepared via RAFT polymerization contain the thiocarbonylthio functionality as the end group. Depending on the application of the product, the group can render the polymer unusable due to its properties such as reactivity or color. Thus, end group modification may be needed to obtain the desired product. Moreover, the recovery of the CTA for use in subsequent reactions is ideal due to the high cost of the compounds. Examples of CTA removal and recovery processes can be found in the literature. Perrier *et al.* reported a method for the recycling of RAFT agents by using free radical initiators.[66] The approach was tested on methacrylate, acrylate, acrylamide and styrenyl polymers prepared with a variety of CTAs. Perhaps the biggest challenge in such post-polymerization processes is the scalability. The detached CTA should be readily recovered without altering the product itself, while keeping the process cost-effective.

3.4. RAFT Emulsion Processes

When the RAFT method was first applied to emulsion systems, considerable difficulties were encountered in controlling molecular weights and achieving colloidal stability.[54] Solutions to various issues were called for before the two techniques were deemed compatible. These problems included transport of the CTA out of the reaction locus, water sensitivity of some CTAs, unsuccessful particle nucleation and rate retardation. Due to the complex interplay of thermodynamic and kinetic effects, the mechanism of RAFT emulsion polymerization is not yet fully understood.[67]

In this context, surface-active CTAs were initially designed to overcome problems related to their water solubility and colloidal instability in *ab initio* syntheses. Such molecules could serve as both the RAFT agent and a surfactant, eliminating the transfer of the CTA in the aqueous phase. They later proved helpful in the synthesis of self-assembling particles in emulsion and dispersion systems. These CTAs include the PEG-based RAFT agents discussed earlier, which have also been studied in emulsion.[68] End-group modification of a hydrophilic PEG chain can give rise to an amphiphilic derivative with surface activity.

However, designing a suitable mCTA is not necessarily straightforward. Rieger *et al.* reported the emulsion polymerization of styrene using a PEG-based dithiobenzoate mCTA.[68] The reaction was slow, and only 26% conversion was achieved after 23 h. Replacing the end group with an alkyl trithiocarbonate gave a 67% conversion in 23 h using similar reaction conditions. Etchenausia *et al.* recently reported the use of a xanthate-terminated PEG chain in an aqueous emulsion copolymerization of *N*-vinylcaprolactam and vinyl acetate.[69] The reaction produced stable latex particles with high dispersities in the absence of coagulum. When PEG was used instead of the mCTA, the reaction produced a large coagulum. This demonstrated the crucial role of the xanthate-terminated PEG in stabilizing the particles.

4. Emulsion Polymerization

Emulsion polymerization is a liquid-phase heterogeneous free-radical polymerization process, in which an insoluble monomer is polymerized in the presence of a stabilizing agent. Today, radical emulsion polymerization is widely used commercially. The advantages of emulsion processes include the ability to have a high polymer content dispersion while maintaining a low viscosity, the ease of heat transfer, and in the case of aqueous emulsion polymerization, the use water as an environmentally friendly dispersing medium. Utilizing the emulsion process, it is possible to attain both a high rate of reaction and a high molecular weight product. This is a significant advantage over homogeneous radical polymerizations, where the degree of polymerization is inversely proportional to the rate of reaction.[55]

4.1. Mechanism of the Emulsion Process

A simplified presentation of the emulsion process is shown in **Scheme 6**. Prior to initiation, an emulsion polymerization system consists of emulsifier-stabilized monomer droplets, monomer-swollen micelles, and the continuous medium with small amounts of molecularly dissolved initiator, monomer, and emulsifier. After an initiating radical is formed in the continuous phase, the addition of monomer units can take place through the diffusion of the radical into a micelle or a monomer droplet, or through propagation in the continuous phase, which will eventually result in precipitation. These three nucleation schemes are known as micellar nucleation, droplet nucleation, and homogeneous nucleation, respectively.[67] As the total surface area of the micelles is much larger than that of the monomer droplets, and due to the poor solubility of the monomer, the polymerization will almost exclusively start in the

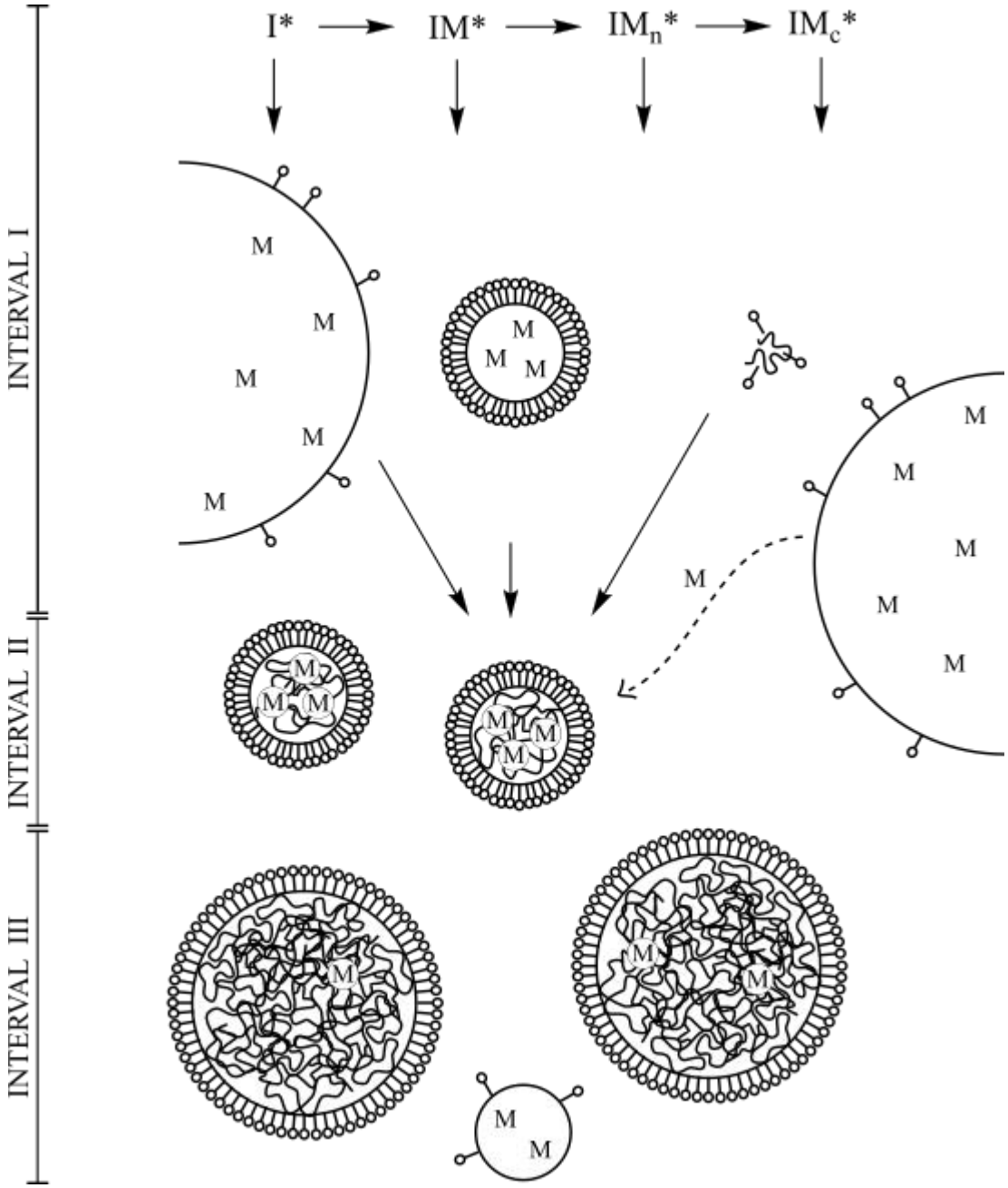

Scheme 6 Schematic representation of emulsion polymerization shows three mechanisms of particle formation and three intervals of reaction.[66] The initiator radical (I*) starts the reaction by adding a monomer in the aqueous phase (IM*) or by entering a monomer droplet or a micelle. It may also propagate (IM_n*) to reach a critical length (IM_c*), at which the chain will become insoluble. The radical can enter a micelle or a droplet at any stage of propagation. Various physical and chemical processes, such as termination reactions and radical exit and re-entry, are not shown.

monomer-swollen micelles.[55] Regardless of the initial nucleation mechanism, instability of the resultant particles will lead to coagulation, giving rise to coagulative nucleation. Micelles with no propagating radicals will provide emulsifier for the stabilization of polymer

particles. This stage of the reaction is characterized by an accelerating reaction rate, resulting from an increasing number density of propagating polymer particle nuclei.

According to the generally accepted kinetics scheme proposed by Harkins[70], the reaction takes place exclusively in the polymer particle phase after particle nucleation is completed. Monomer droplets act as a supply from which more monomer diffuses into the loci of polymerization as it is consumed. The reaction rate remains stable as long as the monomer content of the polymer particles can be replenished. As the monomer droplets become depleted, the monomer concentration in the reaction locus decreases and the reaction rate decelerates. Harkins' theory was later developed into a quantitative description by Smith and Ewart[71].

4.2. Aqueous PISA Formulations

After the development of controlled radical polymerizations, their compatibility with aqueous systems raised interest in utilizing them in emulsion polymerization.[72] On the other hand, among researchers working with emulsion systems, the goal was eventually set to develop surfactant-free emulsion processes. Amphiphilic copolymers were an attractive alternative for low-molar-mass surfactants due to their reduced mobility and enhanced attachment to the particle surface through adsorption and absorption. The two interests were combined when controlled polymerization methods were found to be a potential candidate for producing amphiphilic block copolymers that would stabilize classical latex particles *in situ*.[73] These advances led to the discovery of aqueous emulsion PISA formulations. Today, PISA syntheses are carried out using both aqueous emulsion and dispersion polymerization processes. In dispersion polymerization, the monomer is soluble in the reaction medium, but the growing chain precipitates.

The similarities of conventional aqueous emulsion polymerization and its PISA variant raise a question about the advantages of the two approaches over each other. Perhaps the most apparent advantage of PISA is the possibility to create block copolymer worms and vesicles. Canning *et al.* deemed the conventional method to be superior for the production of near monodisperse spherical particles of 100-1,000 nm diameter.[2] However, PISA formulations seemed more competent for producing spheres of smaller size, as they do not require high amounts of stabilizer. Conventional emulsion systems tend to suffer from excess surfactant, which is also troublesome to remove. Additionally, if sterically stabilized particles are desired, PISA seems preferable to emulsion systems by offering higher blocking

efficiencies.[74,75] It it also worth mentioning that the PISA approach offers a low viscosity option with a faster reaction rate for the solution polymerization of block copolymers.

Although some PISA syntheses have been shown to result in higher order morphologies, such as worms and vesicles, these are mostly seen to be products of aqueous dispersion RAFT reactions.[2] The reason for RAFT aqueous emulsion polymerizations mostly resulting in spherical particles is currently not well understood. For dispersion systems, it is known that the relative volume fractions of the stabilizer and the core-forming block plays an important role in the development of the particle morphology.[76] Long stabilizers promote effective steric stabilization already after nucleation, preventing further sphere-sphere fusion. The fusion is essential for obtaining higher order morphologies. This was illustrated in the work of Blanazs *et al.* where transmission electron microscopy was used to monitor the evolution of the particle shape throughout a PISA reaction.[23] The group prepared poly(glycerol monomethacrylate)-*block*-poly(2-hydroxypropyl methacrylate) copolymers that underwent sphere-to-worm and eventually worm-to-vesicle transitions during the polymerization. Micrographs revealed the presence of hybrid morphologies, such as short worms, partially coalesced worms, and jellyfish, between the more traditional shapes. Such observations provide evidence of the underlying mechanisms. Whereas with conventional self-assembly methods the particle morphologies can be predicted using the packing parameter[9], it has not proved sufficient for predicting the morphologies resulting from PISA reactions. The parameter determines the morphology of the aggregates by relating the volume v and the length l of the hydrophobic segment to the contact area a of the head group as

$$p = v/al\,. \qquad (1)$$

However, such a relationship does not take into account the relative degrees of solvation in the system or the possible concentration dependence.[2] Theoretical advances are needed to better control these reactions.

It should be noted that the use of RAFT not only provides a platform for the syntheses, but also sets boundaries for the outcome. One such limitation is the degree of polymerization. The target length of the resulting polymer in RAFT reactions is given by the monomer-to-CTA ratio. A practical upper limit of monomer concentration means that the chain length can only be increased by decreasing the amount of added CTA. Moreover, the CTA-to-initiator ratio must be kept reasonable to provide a sufficient number of radicals to the

system, while maintaining the livingness of the reaction. Another variable that can pose a problem is the remaining RAFT end-group, which should be either compatible with the application or easily removed by post-polymerization processes. Strategies on end-group removal and recovery can be found in the literature[66], however the self-assembly might result in the end-group being hidden inside the particle and thus poorly accessible for removal. Furthermore, additional steps in the production will increase the costs and decrease the practicality of the technology.

II. EXPERIMENTAL PART

9. Introduction

The aim of this research was to produce a poly(ethylene glycol)-*block*-poly(*N*-vinylcaprolactam) copolymer that would undergo polymerization-induced self-assembly. The plan was to use commercially produced PEG and extend the chain with NVCL units by carrying out the polymerization in an aqueous medium at 50 °C, that is, above the lower critical solution temperature of PNVCL. Several morphologies of polymer particles, such as spheres, worms and vesicles, have been obtained using similar strategies[2]. However, only one research group is known to have exploited the LCST behavior of the growing chain for inducing the self-assembly during polymerization.[8] The resultant morphology could not be predicted, but can be determined using methods such as transmission electron microscopy. The particles were to be physically crosslinked using small molecular weight compounds carrying hydrogen bond donors.

The goal was to carry out the reaction as a controlled radical polymerization, more specifically, as a MADIX-type RAFT polymerization. Therefore, for the polymerization of the PNVCL block, a PEG-based macro-chain transfer agent was required. Poly(ethylene glycol) methyl ether was chosen as the starting material for a two-step synthesis found in the literature, where the hydroxyl end-group was modified into a xanthate moiety. As the result of various PISA reactions were known to be dependent on the volume fractions of the two blocks[2], two different lengths of PEG were chosen for the experiments. Due to the poor water solubility and the melting point of 35-38 °C of NVCL, the reaction was expected to follow the emulsion polymerization mechanism.

To study the system thoroughly, several polymerizations were to be carried out by varying the mCTA length, the initial monomer concentration and reactant ratios. The resultant particles were to be characterized with dynamic light scattering at the reaction temperature before and after physical crosslinking. Dialyzed and dried products were to be analyzed with NMR spectroscopy, size exclusion chromatography, and turbidimetry.

10. Materials

All chemicals were used as received from the supplier unless otherwise stated. Poly(ethylene glycol) methyl ether ($mPEG_{113}$-OH, average M_n 5000), poly(ethylene glycol) methyl ether ($mPEG_{42}$-OH, average M_n ~1900), 2-bromopropionyl bromide (97%), sodium hydroxide (NaOH, ≥ 98%), potassium ethyl xanthogenate (96%), N-(2-Hydroxyethyl)piperazine-N′-(2-ethanesulfonic acid) (HEPES, 99.5%), and Trizma base (Tris, ≥ 99.9%) were purchased from Sigma/Aldrich and used as received. Triethylamine (≥ 99%) was purchased from Merck. Dichloromethane (CH_2Cl_2, 99.99%) was purchased from Fischer Scientific and dried over regenerated 4 Å molecular sieves before use. Diethyl ether (100.0%) and hydrochloric acid (HCl, 37%) were purchased from VWR Chemicals. Magnesium sulfate ($MgSO_4$, anhydrous, > 99.5%) was purchased from Alfa Aesar. *N*-vinylcaprolactam (NVCL, 98%) was purchased from Aldrich and recrystallized twice from toluene prior to use. 2,2'-Azobis[2-(2-imidazolin-2-yl)propane]dihydrochloride (VA-044) was purchased from Wako Chemicals and recrystallized from methanol. Sodium hydrogen carbonate ($NaHCO_3$, 99.9%) was purchased from Fischer Scientific. Dimethylsulfoxide-d_6 (DMSO-d_6, 99.8% D) and deuterium oxide (D_2O, 99.96% D) were obtained from Euriso-Top. Dialysis was conducted using Cellu Sep T1 regenerated cellulose tubular membranes with a nominal MWCO of 3,500.

11. Syntheses

11.1. Preparation of Xanthate-Terminated Macro-Chain Transfer Agents

The mCTAs were prepared from mPEG by adapting a two-step synthesis found in the literature (**Scheme 7**).[6] In the first step, $mPEG_{113}$-OH (20.16 g, 4 mmol) was dissolved in 100 ml of anhydrous CH_2Cl_2 in a dry 250 ml three-necked flask. Triethylamine (1.238 g, 12 mmol) was added and the flask was set in an ice bath. A solution of 2-bromopropionyl bromide (1.3 ml, 12 mmol) in 20 ml of anhydrous CH_2Cl_2 was added dropwise to the solution over 2 h. After the addition, the mixture was taken off the ice and stirring was continued for 1 d.

The solution was filtered and 200 ml of CH_2Cl_2 was added. The organic layer was washed with 1.0 M HCl solution (3 × 80 ml), 1.0 M NaOH solution (3 × 80 ml), and deionized water (2 × 80 ml) and dried with anhydrous $MgSO_4$. The solution was concentrated in a rotary

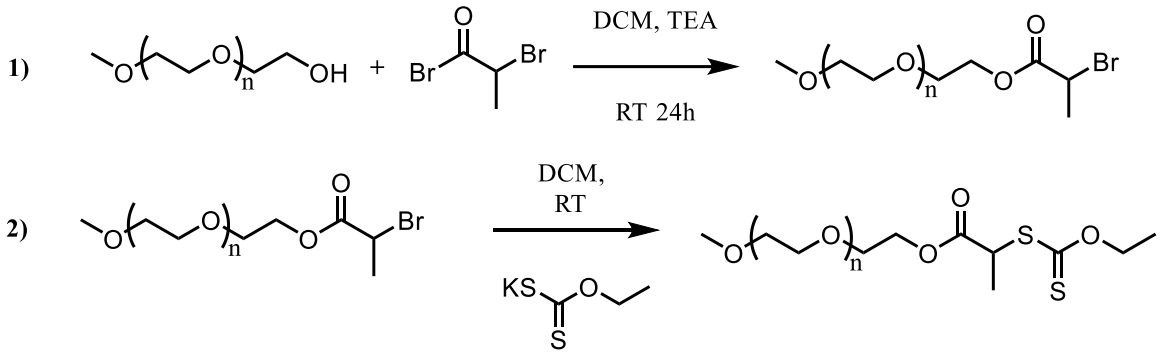

Scheme 7 Synthetic procedure for the preparation of the mCTA used in this work. 1) In the first step, mPEG-OH reacts with 2-bromopropionyl bromide in a base-catalyzed S_N2 reaction to yield an ester, mPEG-Br. 2) In the second reaction, the terminal bromine of the mCTA precursor is replaced by a xanthate moiety, giving mPEG-X.

evaporator at 30 °C to 20 ml. The polymer was precipitated in 400 ml of cold diethyl ether and dried in vacuum for 3 h, giving $mPEG_{113}$-Br. Gravimetric yield: 19.4 g (96%). ^{1}H NMR in DMSO-d_6, 20 mg ml^{-1}.

The same procedure was used for the preparation of $mPEG_{42}$-Br. Gravimetric yield: 89%.

The second step of the synthesis found in the literature was modified, and the resulting procedure was as follows. $mPEG_{113}$-Br (5.00 g, 1 mmol) was dissolved in 100 ml of anhydrous CH_2Cl_2 in a round-bottom flask. Potassium ethyl xanthogenate (0.480 g, 3 mmol) was added. The flask was protected from light and the mixture was stirred for 30 min.

Solids were filtered off and 50 ml of CH_2Cl_2 was added. The solution was washed with saturated $NaHCO_3$ solution (3 × 70 ml) and deionized water (1 × 70 ml). The organic phase was dried with anhydrous $MgSO_4$ and concentrated to 20 ml at 30 °C using a rotary evaporator. The polymer was precipitated in 400 ml of cold diethyl ether. The product was dried under atmosphere overnight. $mPEG_{113}$-X was obtained. Gravimetric yield: 4.64 g (93%). ^{1}H NMR in DMSO-d_6, 20 mg ml^{-1}.

In the preparation of $mPEG_{42}$-X from $mPEG_{42}$-Br, only a 10 min reaction time was used. Longer reaction times seemed to promote difficulties in removing unreacted xanthate from the products, as indicated by impurities in ^{1}H NMR spectra. Gravimetric yield: 90%.

11.2. Polymerization of PEG-b-PNVCL Copolymers

Various aqueous media, concentrations and reactant ratios were used to study the polymerization reaction (**Scheme 8**). The general procedure was as follows. NVCL and mPEG-X were added in a 25 ml two-necked flask. In a separate flask, an excess of VA-044 was dissolved in a small amount of solvent. The needed amount of initiator solution was added in the reaction flask along with the rest of the solvent. The solution was stirred slowly using a magnetic stirrer and bubbled with nitrogen for 1 h at room temperature. A t_0 conversion sample of two drops was taken using a nitrogen-purged syringe. The mixing speed was increased to 400 rpm and the reaction was initiated by immersing the reaction flask in a preheated oil bath. Reaction temperature was 50 ^{o}C. For kinetic studies, conversion samples of two drops were taken through a septum using a nitrogen-purged syringe and quenched with liquid nitrogen.

The polymerization was stopped by opening the system to air and cooling it down with liquid nitrogen. If light scattering experiments were to be conducted on the resultant particles, the reaction was stopped without cooling by only opening the system to air. The system was homogenized by stirring at room temperature before taking the final conversion sample. The reaction mixture was dialyzed against deionized water for 5 d and freeze-dried. ^{1}H NMR in D_2O, 2 drops in 0.6 ml. DOSY in D_2O, 5 mg ml^{-1}.

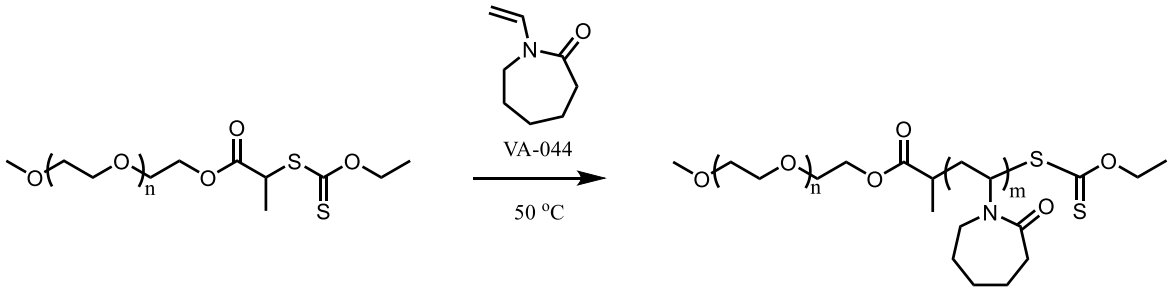

Scheme 8 MADIX polymerization of NVCL.

12. Characterization

12.1. Nuclear Magnetic Resonance (NMR) Spectroscopy

NMR spectra were recorded using a 500 MHz Bruker Avance III spectrometer at 23 ^{o}C. Diffusion-ordered spectroscopy (DOSY) measurements were carried out using the Bruker pulse sequence ledbpgp2s. A diffusion delay of 100 ms was used. Two hours prior to the measurement, a 5 mg ml^{-1} sample was prepared in D_2O. TopSpin and SpinWorks software were used to process the data.

Conversions of the polymerization reactions were determined by the disappearance of the CH_2CHN signal of NVCL.

12.2. Size Exclusion Chromatography (SEC)

SEC analysis was performed on the mCTAs using a Waters 515 HPLC pump connected to a Waters 2410 refractive index detector. Samples of 1 mg ml^{-1} were prepared in an aqueous 0.1 M sodium nitrate solution containing 3% acetonitrile (ACN). Poly(ethylene oxide) (PEO) standards were used for calibration. Separation was attained using a Varian PL aquagel-OH mixed column (100-600,000) and Waters Ultrahydrogel 250 (1,000-80,000) and 120 (100-5,000) columns. Injection volume was 50.0 µl and the elution rate was 0.8 ml min^{-1}. OmniSEC software was used for data analysis.

PEG-*b*-PNVCL samples of 1 mg ml^{-1} were analyzed in THF containing 1 mg ml^{-1} of tetrabutylammonium bromide (TBAB). A Waters ACQUITY APC System was used for the analysis. Poly(methyl methacrylate) (PMMA) standards were used for calibration. Separation was attained with two Acquity APC XT extended temperature columns with 450Å (20,000-400,000) and 200Å (3,00-70,000) pore sizes. Injection volume was 10.0 µl.

Chromatograms were plotted using OriginPro software. Baseline subtraction, normalization and FTT smoothing were used where needed.

12.3. Dynamic Light Scattering (DLS)

DLS measurements were performed using Coherent Sapphire 488-100 CW CDRH as the light source and Brookhaven Instruments' BI-CrossCorr detector, BI-200SM goniometer, and BIC-TurboCorr digital pseudo-cross-correlator. The detector consisted of two BIC-DS1 detectors. The laser operated at 488 nm and 10-15 mW. A 100 µm pinhole and 30-130^{o} angles were used for the measurements. Temperature was controlled using a LAUDA RC 6 CP thermostat.

To conduct the experiment, a sample was withdrawn from the reaction mixture and diluted down in a syringe, while keeping the solution temperature between 50-75 °C. Before beginning the first measurement, the sample was stabilized at 50 °C inside the instrument for 30 min. The measurement was then performed at said temperature. Scattering data was collected for 3 and 10 min for multiple angle and single angle experiments, respectively.

Crosslinking experiment was carried out using saturated aqueous salicylic acid. The solution was prepared at room temperature and filtrated prior to use. After conducting the initial measurements on the polymer particles, salicylic acid solution was heated to 65 °C, and 1 ml was added in the sample cuvette. The cuvette was briefly shaken and left to stabilize in the measuring cell at 50 °C for 15 min before collecting the data.

12.4. Turbidimetry

Turbidity measurements were carried out using a JASCO J-815 circular dichroism spectrometer. The instrument was equipped with an external Peltier PTC-423S/15 temperature control unit. One day prior to the experiment, 1 mg ml^{-1} sample solution was prepared in deionized water. Before starting the measurement, the sample cuvette was kept at 25 °C for 10 min. The spectrum was recorded at a 700 nm wavelength from 25 to 60 °C. The heating rate was 1 °C min^{-1}.

13. Results and discussion

13.1. Preparation of the Macro-Chain Transfer Agents

The purity of the mPEGs used for the mCTA syntheses were determined by ^{1}H NMR. The spectrum of PEG in DMSO-d_6 reveals a hydroxyl peak that does not shift or broaden as a function of concentration or impurities, and can be used for quantitative analysis (**Figures 2** and **3**).[77] The PEG contamination of the starting materials were determined before starting the work, as the presence of PEG in mPEG results in some of the CTA having a xanthate group at both ends of the polymer. The amount of PEG was given by the equation

$$\%\ \mathrm{PEG} = [A_{\mathrm{OH}}/(A_{\mathrm{methoxy}}/3) - 1]/2 \cdot 100, \qquad (2)$$

where A_n is the integral of signal n.[77] The PEG content was found to be 2% for $mPEG_{42}$-OH and 7% for $mPEG_{113}$-OH. The purities were deemed acceptable for the purpose.

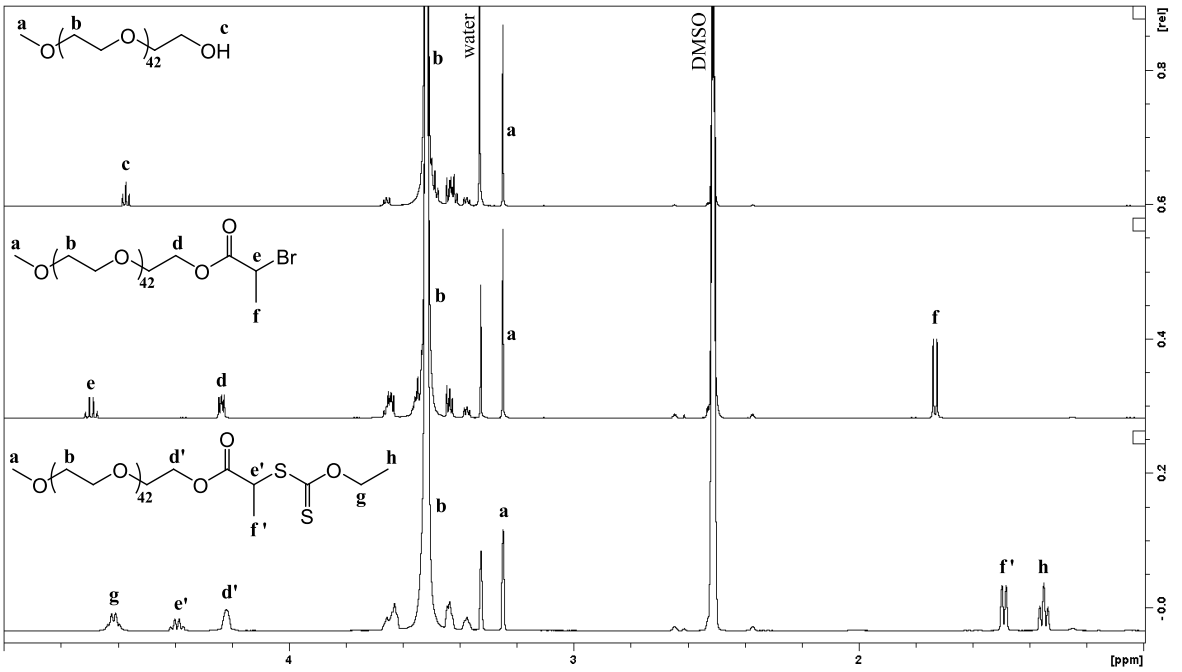

Figure 2 ^{1}H NMR spectra of mPEG$_{42}$-OH (top), mPEG$_{42}$-Br (middle) and mPEG$_{42}$-X (bottom). All spectra were measured in DMSO-d_6 (20 mg ml^{-1}).

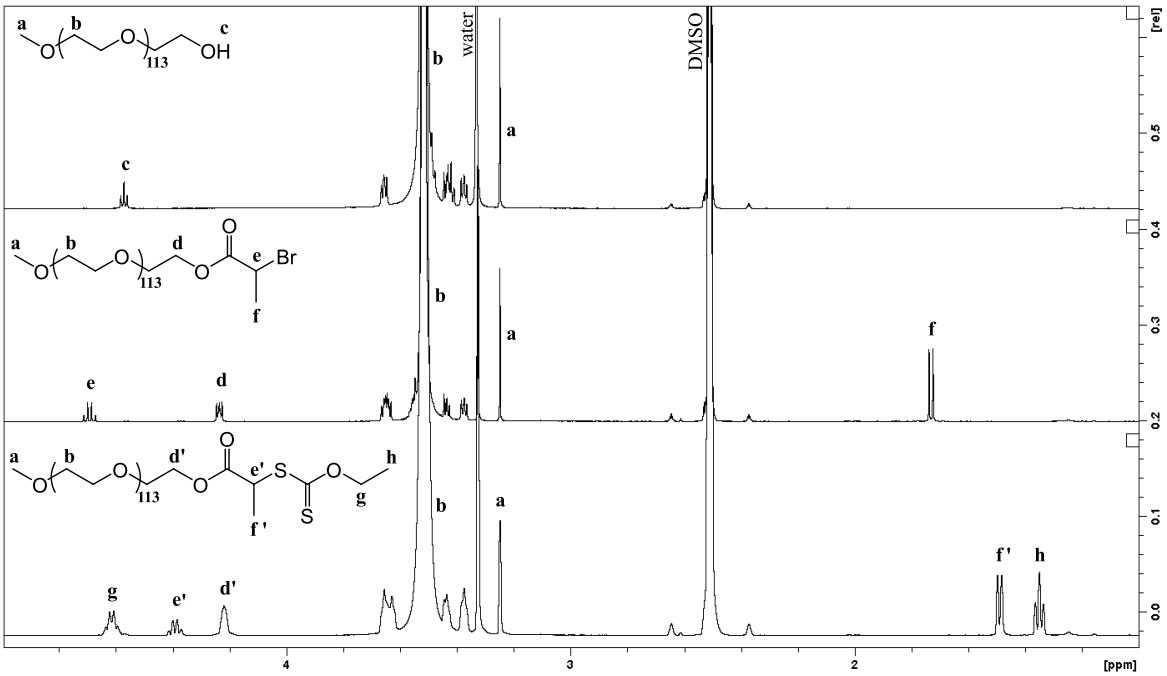

Figure 3 ^{1}H NMR spectra of mPEG$_{113}$-OH (top), mPEG$_{113}$-Br (middle) and mPEG$_{113}$-X (bottom). All spectra were measured in DMSO-d_6 (20 mg ml^{-1}).

The successful syntheses of the mCTAs were demonstrated by ^{1}H NMR measurements. The spectra of $mPEG_{42}$-X, $mPEG_{113}$-X, and their precursors are shown in **Figures 2** and **3** In the first step, full conversion of the hydroxyl end group was confirmed by the disappearance of the triplet arising from the hydroxyl protons at 4.6 ppm. Three new signals arose at 1.7, 4.2 and 4.7 ppm due to the resulting ester. In the second reaction, substitution of the terminal bromine with a xanthate resulted in two new signals at 1.4 and 4.6 ppm, arising from the xanthate protons. Additionally, the chemical shifts of the protons close to the carbonyl group shifted towards lower frequencies due to the new neighboring group.

SEC analysis was conducted to determine the number average molecular weights (M_n) and the dispersities ($Đ_M$) of the CTAs and their precursors (**Table 1**). The analysis was performed in water to get a realistic result with PEO standards, and in THF to later compare the results to those of the copolymers. Due to the poor signal-to-noise ratio of the mPEG-X peaks, the data was smoothed using FFT filtering. This resulted in the baseline resembling a sine wave. However, the visual comparison of the peak shapes was improved significantly. The chromatograms are shown in **Figures 4** and **5**.

For the shorter mCTA, the starting material and the resulting CTA gave clean, symmetric peaks with identical dispersities (**Figure 4**). For $mPEG_{42}$-Br, a smaller compound eluted very close to the polymer. This resulted in partial overlap of the peaks. A likely explanation for this was an unsuccessful purification step. Despite the impurity, the polymer peak could still be seen at its expected position. The peak was analysed by integrating over the estimated

Table 1 SEC analysis of the CTAs and their precursors. [a] Value reported by the supplier. [b] Analyzed in 0.1 M $NaNO_3$ + ACN (3%) using PEO standards. [c] Analyzed in THF + TBAB (1 mg ml^{-1}) using PMMA standards. [d] Analyzed by estimating the integration limit for the polymer peak.

Structure	M_n [a] ($g\ mol^{-1}$)	$M_{n,SEC}$ [b] ($g\ mol^{-1}$)	$Đ_M$ [b]	$M_{n,SEC}$ [c] ($g\ mol^{-1}$)	$Đ_M$ [c]
$mPEG_{42}$-OH	1,900	1,900	1.06		
$mPEG_{42}$-Br		1,900 [d]	1.04 [d]		
$mPEG_{42}$-X		1,900	1.05	3,200	1.13
$mPEG_{113}$-OH	5,000	4,800	1.13		
$mPEG_{113}$-Br		3,000	1.31		
$mPEG_{113}$-X		4,800 [d]	1.07 [d]	9,000	1.16

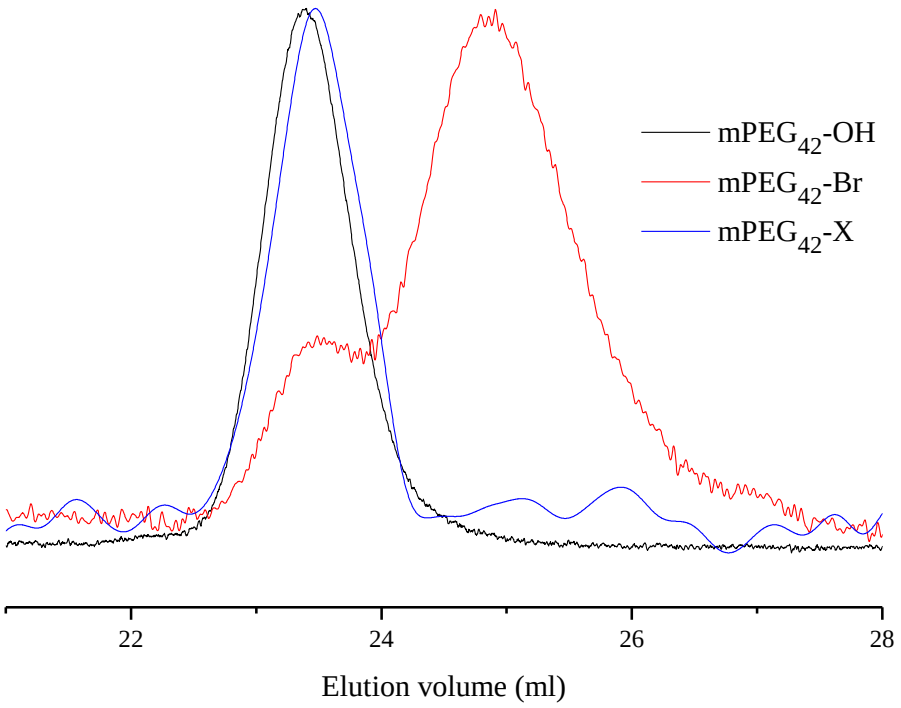

Figure 4 SEC analysis of $mPEG_{42}$-X and its precursors in 0.1 M $NaNO_3$ + ACN (3%) with PEO standards.

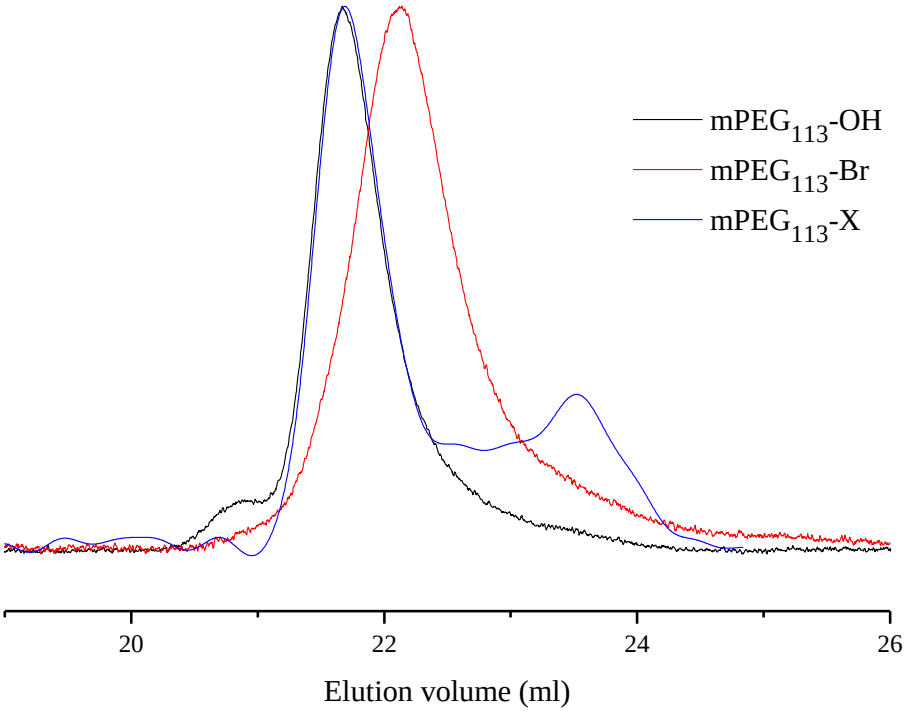

Figure 5 SEC analysis of $mPEG_{113}$-X and its precursors in 0.1 M $NaNO_3$ + ACN (3%) with PEO standards.

polymer peak only. The obtained values of M_n corresponded exactly to that given by the supplier.

In the analysis of the longer mCTA, the starting material eluted close to a small, higher molecular weight impurity (**Figure 5**). The chromatogram exhibited tailing of the peaks for the starting material and $mPEG_{113}$-Br. $mPEG_{113}$-X eluted close to an impurity of a smaller size, which could be an indication of incomplete purification of the product. The peak was analysed by integrating over the product peak only. The molecular weights of $mPEG_{113}$-OH and $mPEG_{113}$-X agreed well with the value given by the supplier. The dispersities of the prepared mCTAs were low, and almost identical. This served as an ideal starting point for the preparation of the block copolymers.

13.2. Polymerization of PEG-b-PNVCL Copolymers

The solubility of NVCL in water is low, approximately 4 g l^{-1}. When an initial monomer content of 4-20 m-% was used for the reactions, the solubility limit was greatly exceeded. Adding the mPEG-X into the reaction mixture seemed to increase the solubility of NVCL slightly. As the melting point of NVCL is 35-38 ^oC, it was hypothesized that the process of polymerizing NVCL in the described system would essentially be emulsion polymerization, and that the reaction would follow emulsion polymerization kinetics.

Before immersing the reaction flasks in an oil bath, there were significant differences in the appearances of the reaction mixtures of different concentrations. When $mPEG_{113}$-X was used, the 4 m-% mixture was a clear solution and no solids remained in the flask. The 8 m-% mixture exhibited small, unstable monomer droplets dispersed in the solvent phase. The formation of such an emulsion at room temperature was unexpected given the melting point of NVCL. A monomer content of 20 m-% resulted in a heterogeneous mixture, as part of the NVCL remained in a solid state until heated. Upon heating the reaction mixtures to 50 ^oC, the solids melted or dissolved for all concentrations. The initial turbidity of the solutions varied from almost clear to nearly milky white. High concentrations promoted increased turbidity.

13.2.1. Effect of the Reaction Medium

Polymerizations of the PEG-*b*-PNVCL copolymers were carried out in deionized water and in aqueous HEPES and Tris buffer solutions. The structures of the buffers are shown in **Figure 6**. The chain extension of $mPEG_{113}$-X with NVCL has been successfully conducted

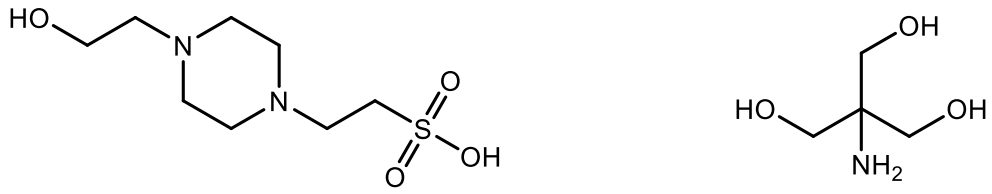

Figure 6 The molecular structure of HEPES (left) and Tris (right).

in DMF by Liu *et al*.[43] In this work, for inducing the self-assembly of the copolymer during the polymerization, aqueous media were used instead. The choice of the reaction medium proved to have a great effect on the results. A similar reaction has been carried out in Tris buffer, utilizing $mPEG_{42}$-X for the copolymerization of vinyl acetate and NVCL.[69]

It should be noted that initially the pH values of the buffer solutions were set to be 7.4 under the reaction conditions. After conducting the experiments, it was found out that Tris and HEPES are highly sensitive to temperature changes.[78] Thus, the pH of the buffer solution was dependent not only on the concentration, but also on the temperature of the solution. As the pH value of Tris was set to 7.4 at 22 °C, the value at 50 °C was approximately 6.6. Similarly, the pH of HEPES was approximately 7.0.

The synthesis of the block copolymer was attempted in deionized water using a high initial monomer concentration (**Table 2**). A comparison between the reactions carried out in water and in Tris revealed a trend for water to promote higher conversions, as suggested by the full disappearance of the double bond protons in the ^{1}H NMR spectra (**Figure 7**). However,

Table 2 A comparison between PEG-*b*-PNVCL polymerization reactions carried out in deionized water and in Tris (0.10 M, pH 6.6). Initial monomer content was 20 m-% for all reactions. [a] Determined by ^{1}H NMR analysis in D_2O.

CTA	Solvent	$[M_0]$:[CTA]:[I]	Yield (%)	Conv. [a] (%)	Reaction time (h)
$mPEG_{42}$-X	H_2O	500:1:1	75	100	24
$mPEG_{42}$-X	Tris	500:1:1	85	94	24
$mPEG_{113}$-X	H_2O	500:1:1	70	100	23
$mPEG_{113}$-X	Tris	500:1:0.3	91	99	24

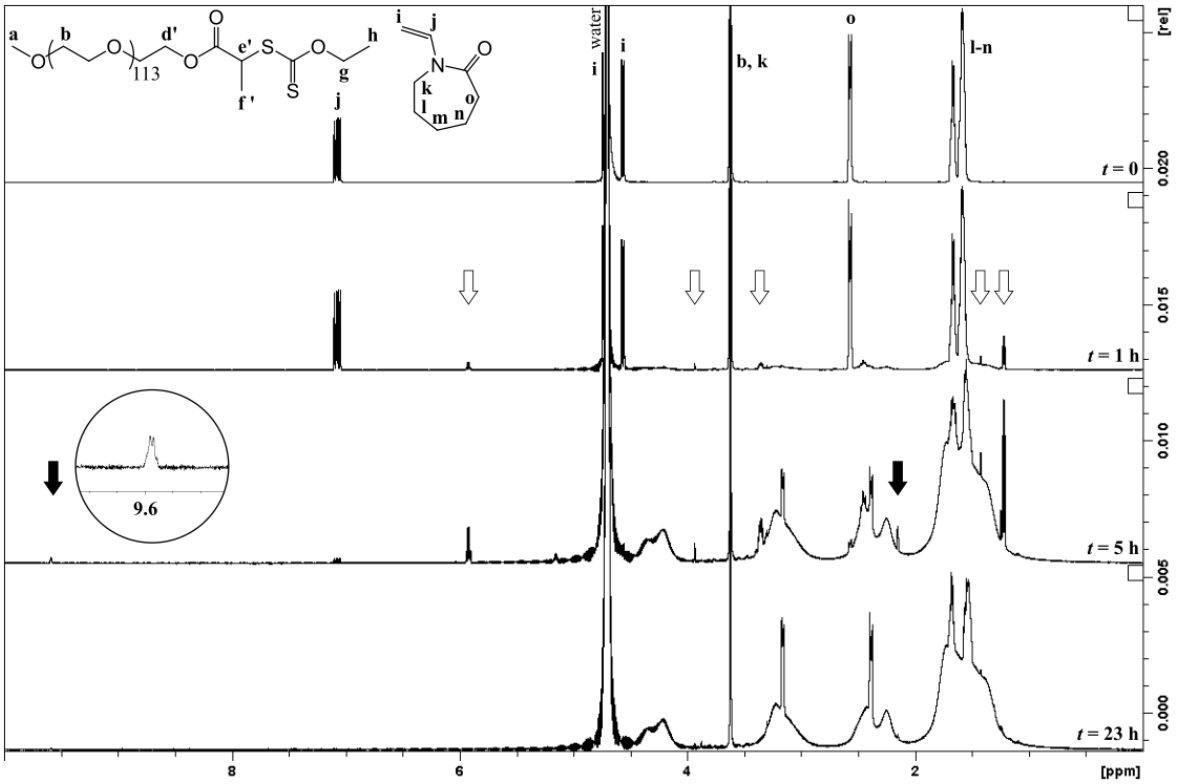

Figure 7 ^{1}H NMR conversion spectra for the 20 m-% reaction utilizing mPEG$_{113}$-X in deionized water. Arrows indicate the signals that are not seen when the reaction is carried out in Tris buffer. Signals indicated by the black arrows correspond to the chemical shifts of acetaldehyde.[79] The spectra were measured from 2 drops of reaction mixture in 0.6 ml of D_2O.

despite the seemingly higher conversions, gravimetric yields were significantly lower for the water reactions than for their Tris counterparts.

A possible explanation for the observations was the hydrolysis of NVCL. The process has been shown to take place as a result of increasing acidity of the reaction medium in systems where potassium persulfate was used as an initiator.[79] The mechanism suggested in the literature produces acetaldehyde and caprolactam. The conversion spectra of the 20 m-% reaction with mPEG$_{113}$-X in deionized water showed the appearance and disappearance of signals that were not present when the reaction was carried out in Tris. An in-depth analysis of the spectra revealed possible acetaldehyde and caprolactam peaks. The signals seen at 9.6 and 2.2 ppm corresponded to those designated to acetaldehyde in the literature.[79] The absence of the >N*H* signal of caprolactam could be explained by the exchange of protons with the deuterated solvent. Furthermore, the peak shapes at 23 h reaction time suggested that not all caprolactam rings were incorporated in a polymeric structure.

The ^{1}H NMR data indicated that instead of all the NVCL taking part in the polymerization reaction, the apparent 100% conversions in water were partially a result of the hydrolytic cleavage of the vinyl group. The side reaction could be further investigated by using other deuterated solvents to maintain the exchangeable protons in the spectra. However, for this work, the nature of the side reaction was not important. It was concluded that deionized water was not an optimal reaction medium, and that the use of a buffer solution was a requirement to have a good control over the reaction.

The polymerization was attempted in HEPES solution to better control the reaction conditions. HEPES is a biocompatible zwitterionic buffer with a pK_a of 7.4 at 20 °C.[80] Two reactions were carried out using mPEG$_{42}$-X and an initial monomer content of 4 m-% (**Table 3**). The conversions were extremely low compared to the conversion achieved in Tris solution using the same mCTA and concentration. ^{1}H NMR showed a 3% conversion for both HEPES reactions. The conversions correlated well with the amounts of solids obtained, which confirmed that barely any reaction was taking place.

The poor conversions were explained by the tendency of HEPES to form radicals.[81] The formation of radicals has been shown to take place in various buffers containing a piperazine ring. These radicals have half-lives of approximately 10 min, which makes them sufficiently stable to prevent any radical polymerization from taking place in the aforementioned conditions. After these findings, it was concluded that the low conversions were a result of chain transfer to HEPES. The participation of the buffer in radical reactions makes it an undesirable buffer candidate for any radical polymerization.

Polymerizations were conducted in Tris buffer. Tris is frequently used in biochemistry due to its low cost and high buffer capacity. Some disadvantages of the buffer include the reactivity of the amine group and its toxicity for many mammalian cells due to its high

Table 3 A comparison between PEG-*b*-PNVCL polymerizations carried out in HEPES (10 mM, pH 7.0) and in Tris (0.10 M, pH 6.6) solutions. The initial monomer content was 4 m-% for all reactions. [a] Monomer conversion determined by ^{1}H NMR analysis in D_2O.

CTA	Solvent	[M_0]:[CTA]:[I]	Yield (%)	Conv. [a] (%)	Reaction time (h)
mPEG$_{42}$-X	HEPES	500:1:0.3	2	3	24
mPEG$_{42}$-X	Tris	500:1:0.3	67	78	24
mPEG$_{42}$-X	HEPES	500:1:1	1	3	24

lipophilicity. Multiple reactions were carried out using an initial monomer content of 4-20 m-%. Experimental data shows Tris to be a suitable buffer for conducting the polymerization (**Table 4**). Conversions of the reactions were high and gravimetric yields correlated well with the conversions. The small difference was due to loss of product during the purification process. The buffer seemed to prevent any unwanted side reactions, as indicated by the ^{1}H NMR conversion spectra (**Figure 8**). The reason for the low conversion of the 4 m-% reaction with mPEG$_{113}$-X was not clear, as the reaction with mPEG$_{42}$-X gave a relatively high yield.

13.2.1. Effects of Stabilizer Length and Monomer Concentration

The most significant difference between the reactions carried out using different lengths of mCTA was the stability of the resulting particles. The use of the shorter stabilizing block resulted in aggregation of the polymer in the reaction mixture. The aggregates were sticky and thus prevented magnetic stirring for the remainder of the reaction time. Such reaction conditions were clearly unsuitable for the purpose, and the reactions were considered unsuccessful. The longer stabilizing block allowed for the preparation of stable particles that were not soluble in water at the reaction temperature. The reactions at high concentrations resulted in a milky white colloid that turned into a clear solution upon cooling (**Figure 9**).

Table 4 Parameters of the PEG-*b*-PNVCL polymerization reactions performed in Tris solution (0.10 M, pH 6.6). [a] Stability of the resulting particles. Stable (S) mixtures had no coagulum at the end of the reaction. Unstable (U) mixtures exhibited aggregation of the latex. [b] Monomer conversion determined by ^{1}H NMR analysis in D_2O.

CTA	M_0 (m-%)	[M_0]:[CTA]:[I]	Stability [a]	Yield (%)	Conv. [b] (%)	Reaction time (h)
mPEG$_{42}$-X	4	500:1:0.3	U	67	78	24
	6	500:1:0.3	U	69	79	18
	8	500:1:1	U	74	86	18
	10	500:1:0.3	U	73	85	21
	20	500:1:1	U	85	94	24
mPEG$_{113}$-X	4	500:1:0.3	S	6	9	24
	8	500:1:0.3	S	66	84	23
	10	500:1:0.3	S	97	97	26
	20	500:1:0.3	S	91	100	24

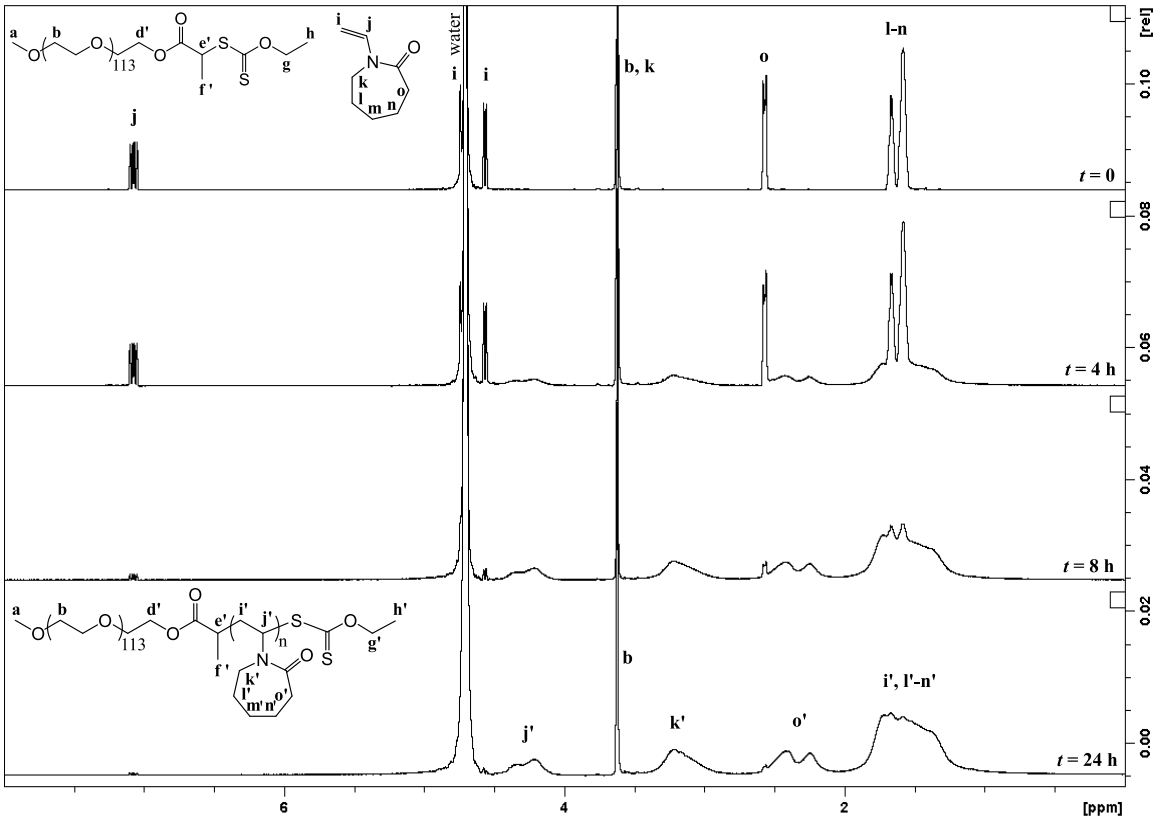

Figure 8 ^{1}H NMR spectra of the 20 m-% reaction in Tris (0.10 M, pH 6.6) using mPEG$_{113}$-X as the mCTA. The spectra were measured from 2 drops of reaction mixture in 0.6 ml of D_2O.

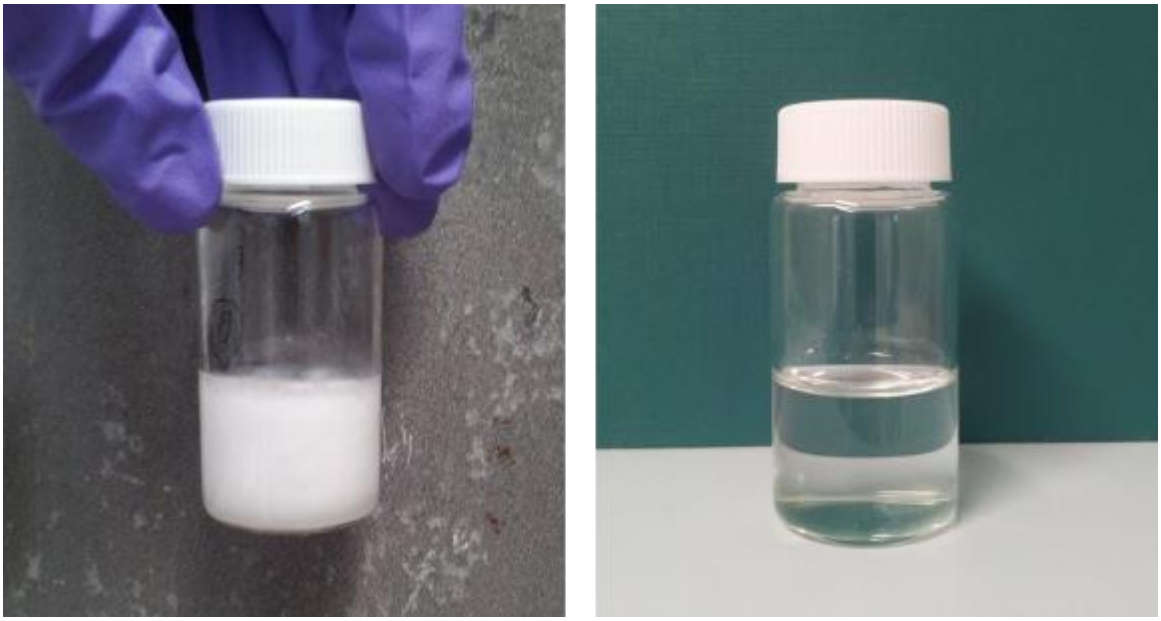

Figure 9 Polymerization product of a 10 m-% reaction with mPEG$_{113}$-X at 50 °C (left) and after cooling to room temperature (right).

The 10-20 m-% reactions with $mPEG_{113}$-X were deemed as successful PISA reactions due to their good particle stabilities and high conversions.

The molecular weights of the dialyzed and freeze-dried products were estimated by ^{1}H NMR and SEC (**Table 5**). The theoretical values of M_n were systematically greater but corresponded well to those given by spectroscopic and chromatographic techniques. Possible sources of error were the use of PMMA standards, as well as heterogeneity of the dried polymer samples. The good correlation between the theoretical and the experimental molecular weights suggested a controlled character of the reaction.

Chromatograms of the SEC analyses are shown in **Figures 10** and **11**. The unstable particles prepared using the shorter stabilizer revealed two types of products (**Figure 10**). The copolymers prepared at low initial monomer concentration showed peaks with a broad shoulder on the low-molecular-weight side of the distribution. With increasing concentration, the shoulder was seen to grow bigger. For the 10-20 m-% reactions it represented the majority of the product, with a smaller overlapping peak seen at the high-molecular-weight side of the distribution. However, the highest molecular weight of the distribution was the same for every reaction. All peaks extended over the mCTA elution area, being a possible indicator of unreacted mCTA. All products exhibited high dispersities.

Table 5 Molecular weights, dispersities and cloud-point temperatures of the prepared copolymers. The reactions correspond to those presented in **Table 4**. [a] Calculated as M_{mPEG} + conv. × [M_0] / [CTA] × M_{NVCL}. [b] Estimated by ^{1}H NMR analysis in D_2O. [c] Analyzed in THF + TBAB (1 mg ml^{-1}) using PMMA standards. [d] Calculated as conv. × [M_0] / [CTA]. [e] Determined by turbidimetry in water and defined as the temperature at which the transmittance started to decrease.

CTA	M_0 (m-%)	$M_{n,theor.}$ [a] (g mol^{-1})	$M_{n,NMR}$ [b] (g mol^{-1})	$M_{n,SEC}$ [c] (g mol^{-1})	$Đ_M$ [c]	$DP_{theor.}$ [d]	T_c [e] (°C)
$mPEG_{42}$-X	4	56,400	49,500	46,200	3.22	390	
	6	57,100	49,300	56,200	3.06	395	
	8	61,900	52,500	45,200	3.48	430	
	10	61,200	57,800	40,900	3.20	425	
	20	67,500	57,500	46,500	2.74	470	
$mPEG_{113}$-X	4	11,400	6,100	9,100	1.15	45	
	8	63,600	56,400	54,500	2.60	420	34.1
	10	72,700	67,100	68,300	2.04	485	34.5
	20	74,800	68,700	67,800	1.68	500	35.2

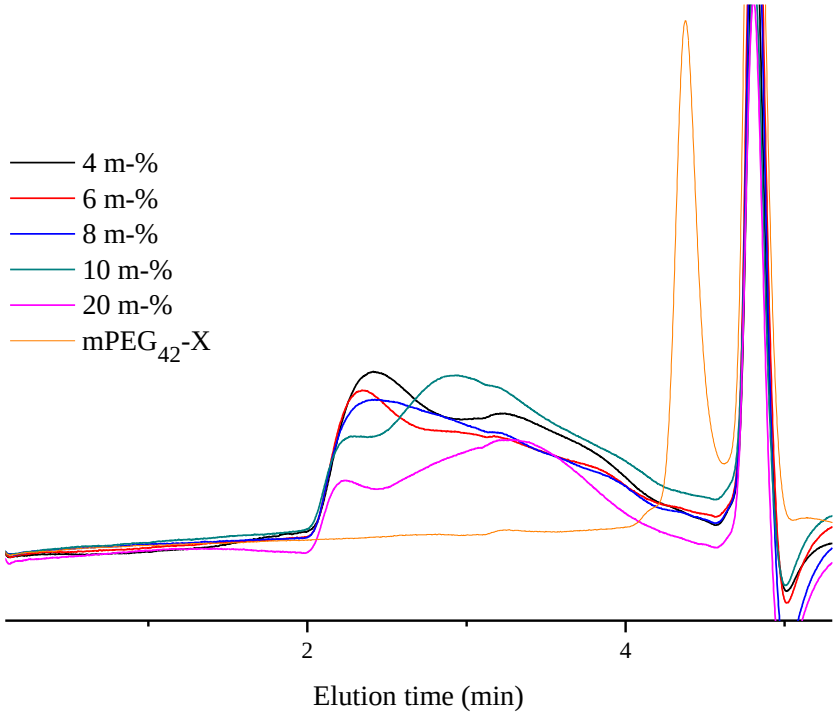

Figure 10 SEC traces of PEG_{42}-*b*-PNVCL copolymers and the corresponding CTA. The analysis was conducted in THF containing TBAB (1 mg ml^{-1}) using PMMA standards.

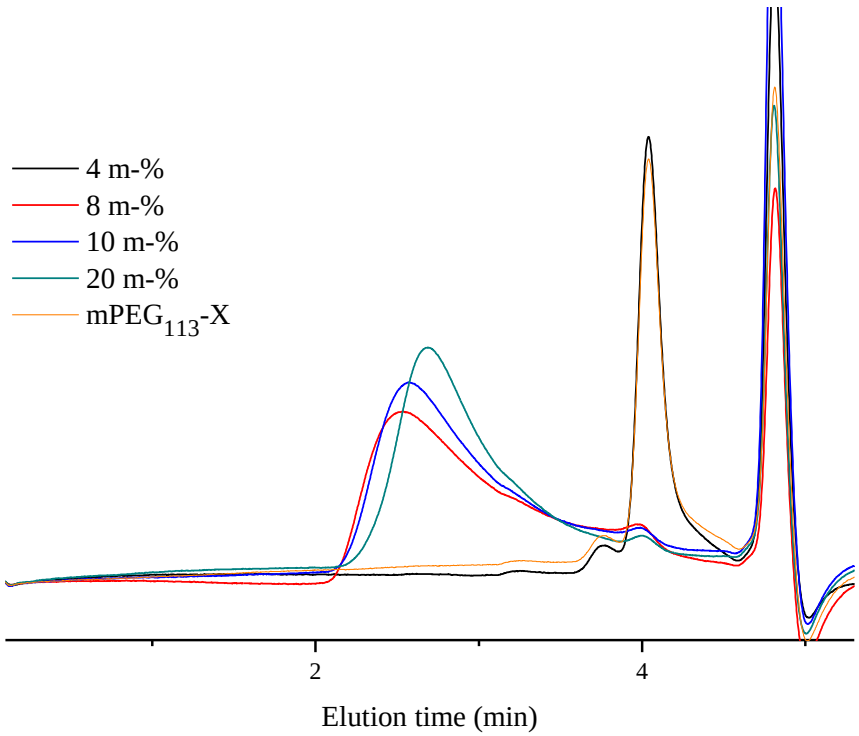

Figure 11 SEC traces of PEG_{113}-*b*-PNVCL copolymers and the corresponding CTA. The analysis was conducted in THF containing TBAB (1 mg ml^{-1}) using PMMA standards.

Polymerizations using $mPEG_{113}$-X yielded products with broad molecular weight distributions (**Figure 11**). However, the shape of the peaks for the 8-20 m-% reactions were much preferable to those presented earlier. Furthermore, the dispersity decreased significantly with increasing reaction concentration. All samples were seen to contain unreacted mCTA. The heterogeneity of the product was possibly a result of the complexity of the RAFT emulsion system. The chromatogram of the 4 m-% product corresponded almost perfectly to that of pure mCTA, confirming that barely any reaction took place during polymerization.

The formation of a block copolymer was further studied by DOSY measurements in D_2O. The data was plotted on an xy-plane, where x represents the chemical shift and y is the logarithm of the diffusion coefficient. Spectra were recorded for $mPEG_{113}$-X and the polymerization product of a 20 m-% reaction with said mCTA. This allowed for the investigation of any possible changes in the diffusion coefficient of the PEG chain as a result of the reaction.

The DOSY spectrum of the block copolymer (**Figure 12**) showed a diffusion coefficient of $3.6 \cdot 10^{-11}$ m^2 s^{-1} for the PNVCL block and a slightly higher average value of

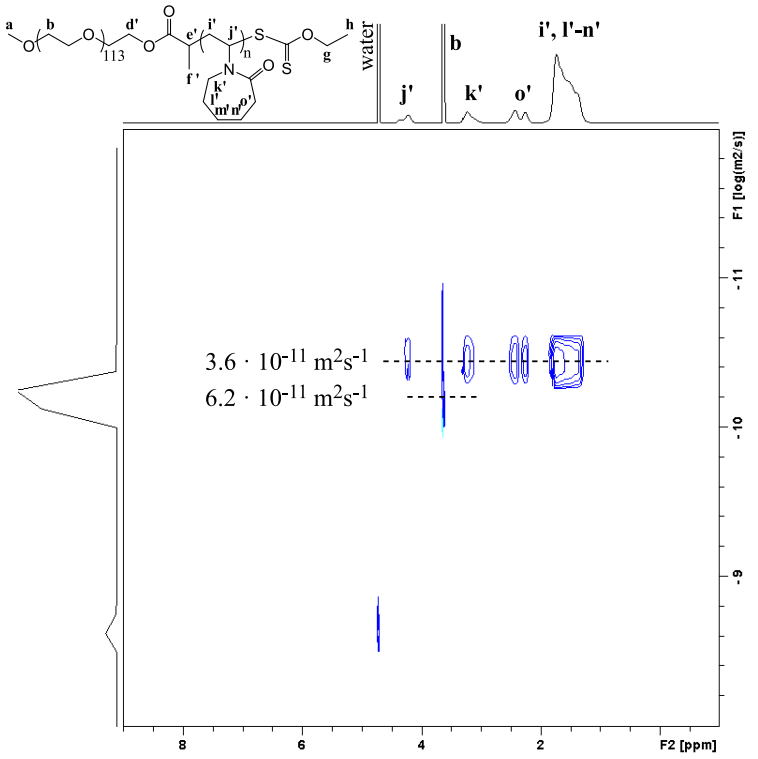

Figure 12 DOSY NMR spectrum of PEG_{113}-*b*-PNVCL in D_2O (5 mg ml^{-1}).

$6.2 \cdot 10^{-11}$ m^2 s^{-1} for the PEG block. In the spectrum of $mPEG_{113}$-X (**Figure 13**), all signals were aligned and exhibited a diffusion coefficient of $1.0 \cdot 10^{-10}$ m^2 s^{-1}. Thus, the average diffusion coefficient of the PEG block of the copolymer was somewhere between those of pure $mPEG_{113}$-X and the PNVCL block. The result confirmed the presence of unreacted mCTA in the sample. More importantly, it suggested that some of the PEG was incorporated in the product, and that the RAFT agent had taken part in the reaction.

Turbidimetry measurements were used to determine the cloud point temperature (T_c) of the purified polymers (**Figure 14**). The experiment was only conducted on the products of the 8-10 m-% reactions with a long stabilizer. The obtained transmittance spectra exhibited a sudden increase in turbidity as the phase transition region was reached. The spectra revealed a trend where the transition temperature increased with increasing polymerization concentration. Thus, the obtained $M_{n,SEC}$ values suggested that the transition temperature increased with increasing molecular weight. Such results were not in an agreement with the literature.[43] A closer look at the SEC data revealed that the trend seen in the transmittance measurements correlated well with the upper limits of the molecular weight distributions. In other words, the transmittance begun to decrease as the longest chains of the sample became

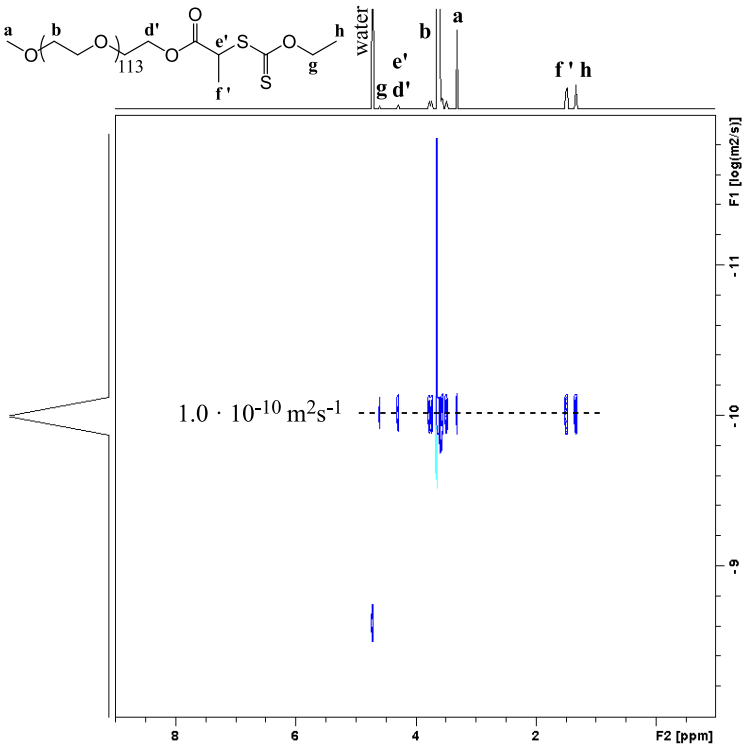

Figure 13 DOSY NMR spectrum of $mPEG_{113}$-X in D_2O (5 mg ml^{-1}) shows an apparent diffusion coefficient of $1.0 \cdot 10^{-10}$ m^2 s^{-1}.

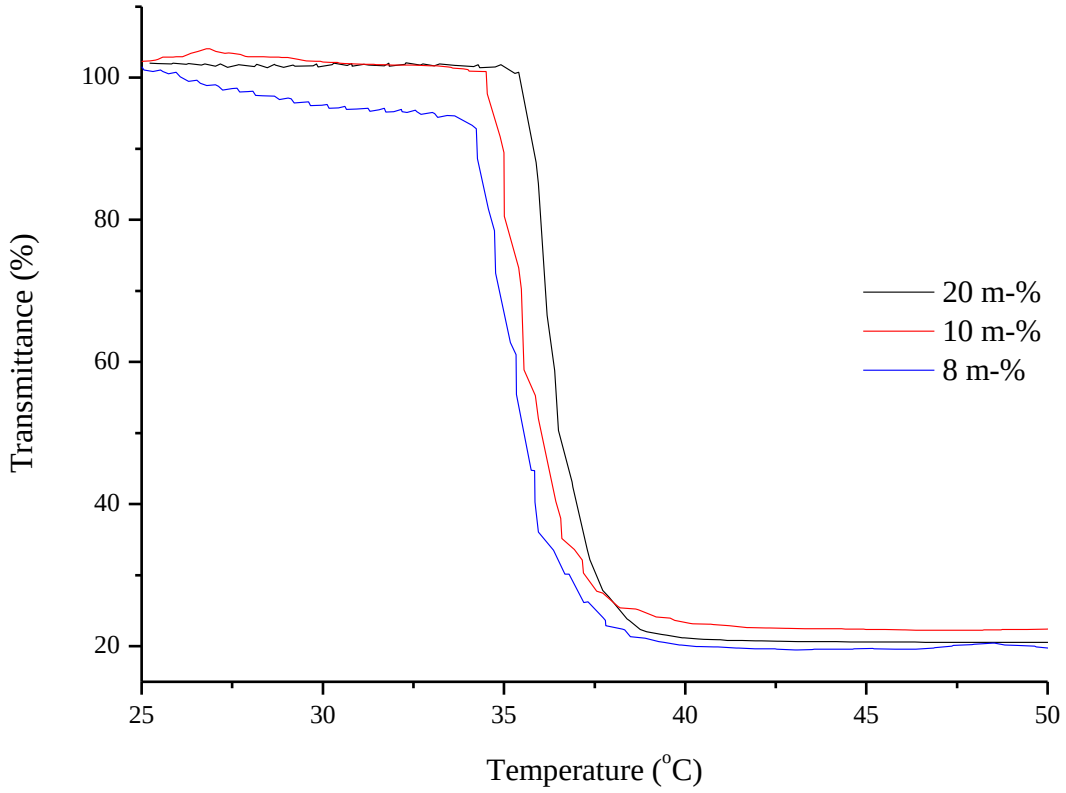

Figure 14 Transmittance spectra of PEG_{113}-*b*-PNVCL copolymers in water (1 mg ml^{-1}).

insoluble. The transition temperatures of the 8 and 10 m-% reactions were close to each other, much as the highest molecular weights they contained, as seen from the chromatograms. The 20 m-% product contained only shorter chains, and thus exhibited a higher T_c.

Dynamic light scattering experiments were conducted on three successful PISA products to determine their particle size distributions (**Table 6**). Data was collected for 10 min at a 90°

Table 6 Products characterized by dynamic light scattering. $mPEG_{113}$-X was used for all reactions. [a] Determined by ^1H NMR analysis in D_2O.

M_0 (m-%)	$[M_0]$:[CTA]:[I]	Conv. [a] (%)	$M_{n,NMR}$ [a] (g mol^{-1})	Mean R_h (nm)
20	500:1:0.3	100	69,300	102
10	500:1:0.3	97	67,100	104
10	350:1:0.3	97	50,800	95

angle and analyzed using the CONTIN algorithm. The correlation functions of all measurements showed monomodal decay (**Figure 15**). The single exponential behavior was better demonstrated by the linearity of the natural logarithm. The correlation functions of the 500:1:0.3 feed products seemed almost identical. The corresponding histograms showed the distributions of the hydrodynamic radii (R_h) to be narrow for all samples (**Figure 16**), however the 350:1:0.3 feed resulted in a slightly broader particle size distribution than the 500:1:0.3 feed. Mean hydrodynamic radii were seen to correlate with the molecular weights determined by ^{1}H NMR analysis. Multiple angle measurements were conducted on the samples to study the angular dependence of the particle size. **Table 7** shows the data collected before and after physical crosslinking. The data was analyzed using both the CONTIN algorithm and the cumulant method. As the initial experiments showed monomodal size distribution of the particles, the cumulant expansion was deemed as a reliable analysis method. The method assumes a Gaussian-like distribution of the particles, which was true for all samples based on the presented histograms. The relative standard

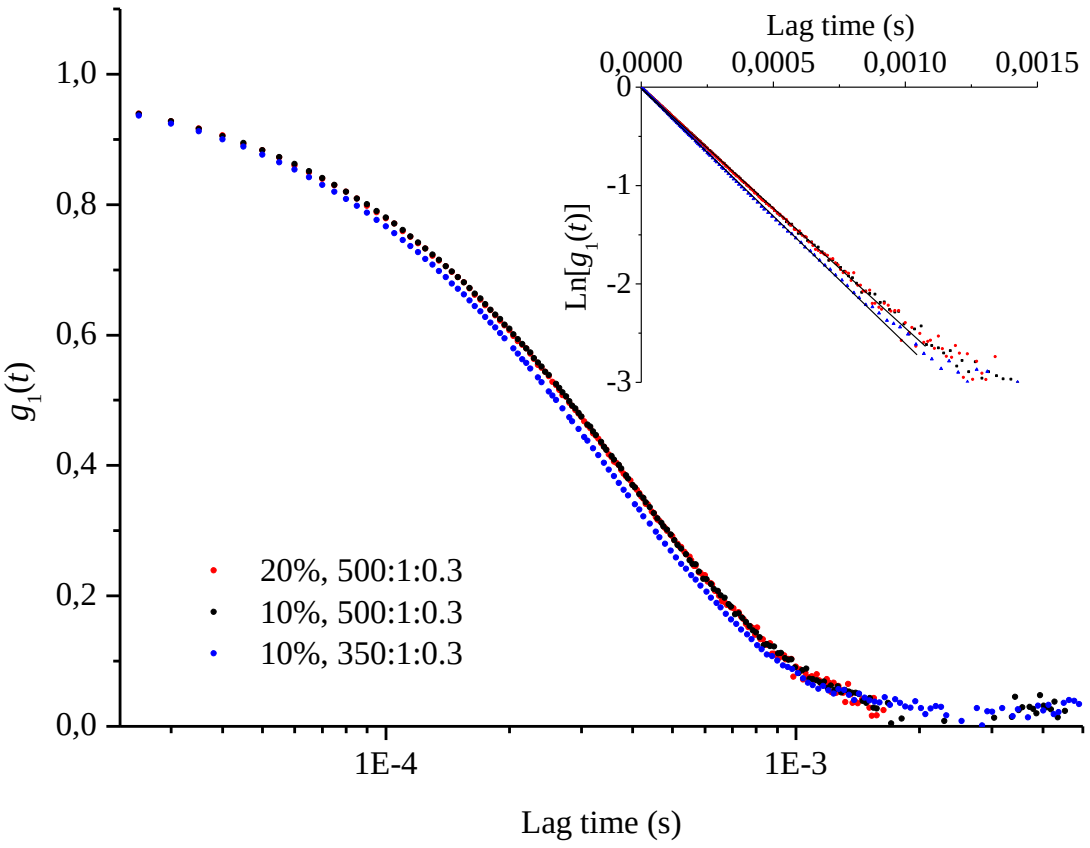

Figure 15 Normalized correlation functions of the scattered light intensity. Monomodal decay was seen for all series of data, indicating monomodal particle distributions.

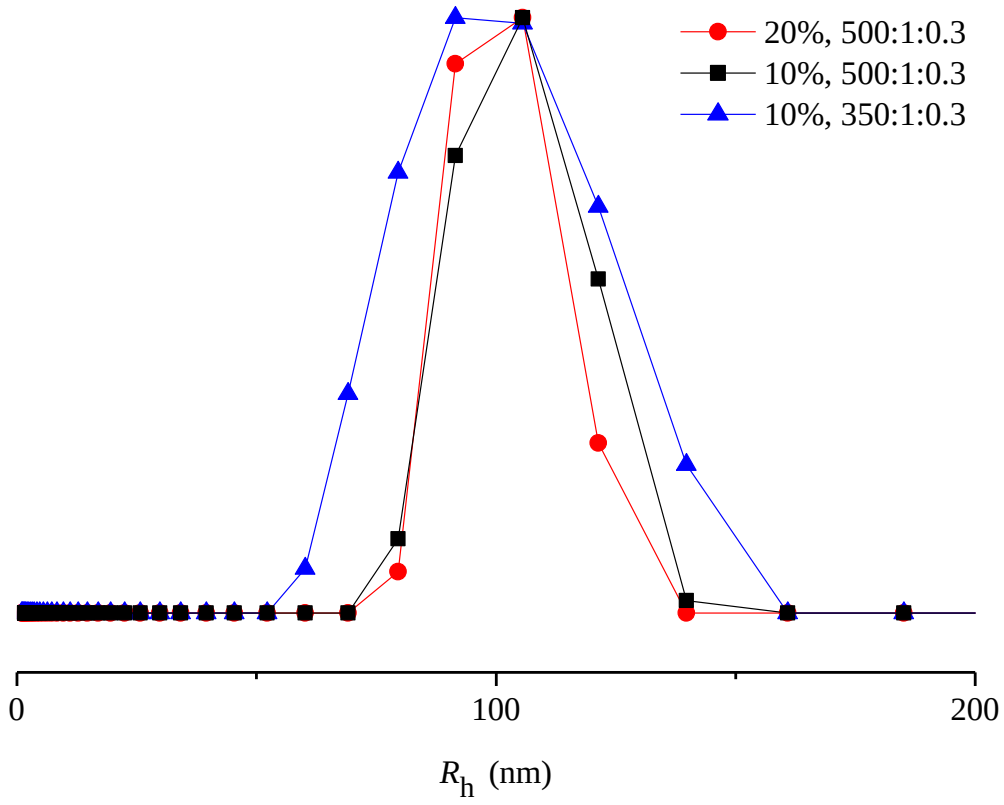

Figure 16 Normalized distributions of the hydrodynamic radii of PISA products. The histograms correspond to the data presented in **Figure 15.**

deviation (RSD) of effective R_h was exceptionally low for the 10 m-% reaction utilizing a 350:1:0.3 feed. The RSD varied between 0.4-8.7% for all samples, confirming that the presented polymerization method is suitable for producing particles with well-defined sizes. Dispersities varied between 0.005-0.184, and tended to increase with decreasing detection angle. Smallest variation was seen for the 20 m-% reaction.

Preliminary crosslinking experiments were conducted on one of the samples to study the possibility of maintaining the particle shape at ambient temperatures. PNVCL particles can be physically crosslinked using a small-molecular compound containing hydrogen bond donors.[10] For this purpose, saturated salicylic acid solution was added in the sample cuvette after conducting the initial DLS measurements. The results showed that the crosslinking did not affect the particle size. The crosslinked particles did not dissolve upon cooling to room temperature. Few aggregates were seen in the cuvette, most likely due to temperature gradients during the addition of the crosslinker.

Table 7 Data analysis of the multiple angle experiment of the PISA particles at 50 °C.

			BEFORE PHYSICAL CROSSLINKING			AFTER PHYSICAL CROSSLINKING		
			CONTIN	2nd cumulant		CONTIN	2nd cumulant	
M_0 (m-%)	[M_0]:[CTA]:[I]	Angle (°)	Mean R_h (nm)	Eff. R_h (nm)	Poly	Mean R_h (nm)	Eff. R_h (nm)	Poly
20	500:1:0.3	30	136.55	127.55	0.072			
		60	111.25	112.35	0.019			
		90	99.30	101.35	0.020			
		120	96.95	106.70	0.005			
Mean			111.01	111.99				
SD			15.71	9.79				
RSD (%)			14.2	8.7				
10	500:1:0.3	30	110.10	116.35	0.110	114.55	114.55	0.052
		40	143.05	114.95	0.050			
		50	111.05	113.20	0.022	110.65	109.50	0.046
		70	107.10	105.35	0.048	125.45	103.20	0.022
		90	99.55	101.60	0.005	95.80	99.60	0.020
		110	98.00	101.75	0.005	92.95	98.85	0.006
		120	102.00	105.75	0.005			
		130	104.55	107.45	0.005	102.65	102.90	0.044
Mean			109.43	108.30		107.01	104.77	
SD			13.44	5.13		11.20	5.56	
RSD (%)			12.3	4.7		10.5	5.3	
10	350:1:0.3	30	90.50	94.55	0.184			
		40	84.15	93.85	0.111			
		50	102.80	94.40	0.092			
		60	93.15	94.80	0.050			
		70	99.20	94.90	0.082			
		80	98.75	94.55	0.045			
		90	117.00	94.70	0.023			
		120	93.85	94.25	0.008			
		130	116.80	93.85	0.045			
Mean			99.58	94.43				
SD			10.57	0.36				
RSD (%)			10.6	0.4				

13.2.2. Reaction Kinetics

Conversion sampling was carried out for four reactions to study them in more depth (**Table 8**). The effects of concentration and reactant ratios become especially important when the procedure is used to pursue various morphologies of the resultant polymer particles. It is known that for some systems the resulting morphology depends on the relative volume fractions of the soluble and insoluble blocks[82], and even on the total solids concentration[76]. Additionally, for light scattering experiments, it was essential that only minimal monomer residue was left in the reaction mixture, as the product could not be purified before the measurements. Any remaining insoluble NVCL can form droplets in water at 50 °C and act as a source of error in the measurements. Thus, a full conversion is desirable.

For the first comparison, 10 and 20 m-% reactions were carried out using identical feed ratios. The conversion data revealed that the higher concentration promoted a significantly faster reaction rate (**Figure 17**). The 20 m-% reaction reached a constant rate period soon after initiation. The conditions allowed for the reaction to reach an 80% conversion before deceleration of the reaction rate took place. The final conversion was achieved only within 13 hours of initiation. The 10 m-% reaction reached its linear region within four hours. The biggest differences in the curves were seen after said point. A lower concentration resulted in a gentler slope in the linear region and a significantly longer deceleration period. The latter constituted for over half of the reaction time required to reach full conversion. The conversion profiles of the reactions resembled much of those often presented for emulsion polymerization systems.[55] The data exhibited three intervals of reaction, representing particle nucleation, particle growth and finally depletion of the monomer droplets.[67]

Table 8 Effect of the concentration and reactant ratios on the reaction rate and conversion. All reactions were carried out in Tris buffer (0.10 M, pH 6.6) using $mPEG_{113}$-X. [a] Time required to reach the interval. [b] Time required to reach end conversion. [c] Determined by ^1H NMR analysis in D_2O.

M_0 (m-%)	$[M_0]$:[CTA]:[I]	Yield (%)	t_{II} [a] (h)	t_{III} [a] (h)	$t_{conv.}$ [b] (h)	Conv. [c] (%)	Reaction time (h)
20	500:1:0.3	90	2.5	5.5	12.5	98	24
10	500:1:0.3	91	5.5	10.0	24.5	97	26
10	350:1:0.3	87	4.5	9.0	22.5	97	24
10	200:1:0.3	97	3.5	8.5	18.0	97	20

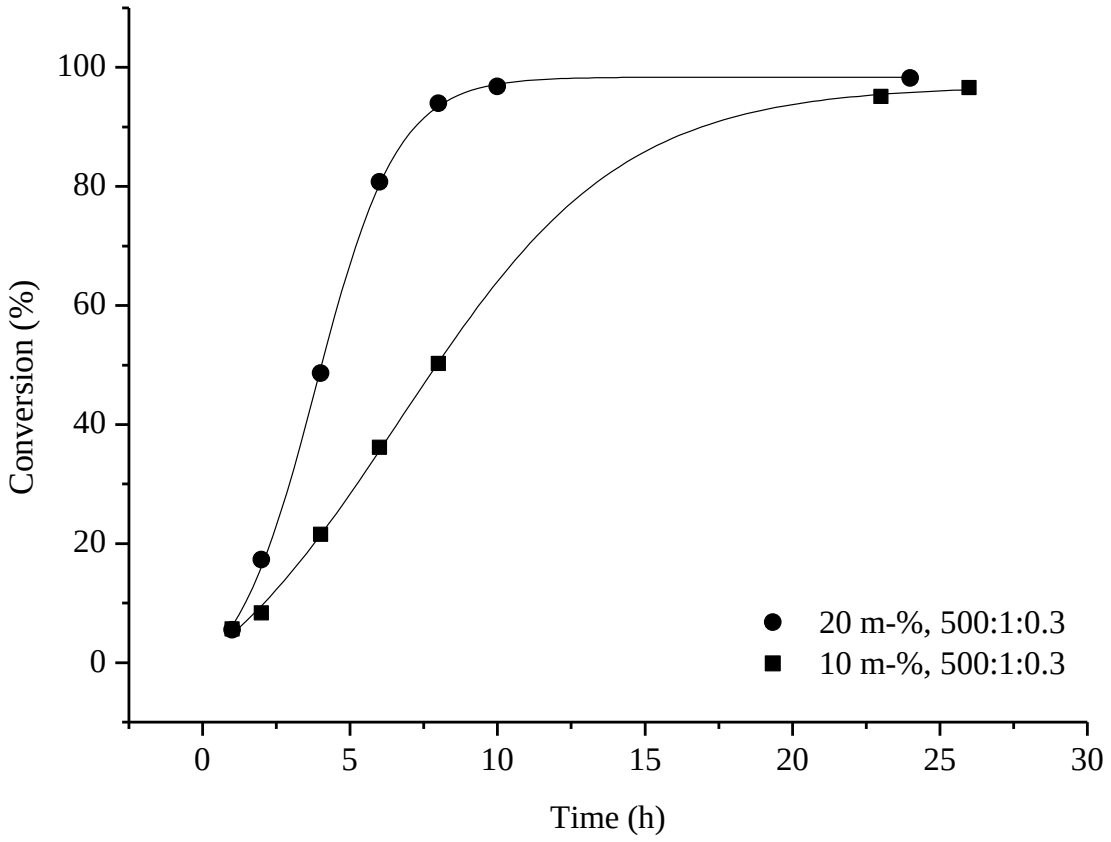

Figure 17 Evolution of the conversion in the polymerization of NVCL. $mPEG_{113}$-X and $[M_0]$:[CTA]:[I] of 500:1:0.3 were used for both reactions. Conversion was determined by ^1H NMR analysis (2 drops of reaction mixture in 0.6 ml of D_2O).

For the second comparison, the kinetics of three 10 m-% reactions with different reactant feeds were compared to each other. The reactant ratios were kept typical for a RAFT polymerization. It was seen that decreasing the initial amount of monomer relative to the amount of CTA and initiator resulted in faster reaction rates (**Figure 18**). It is known that in emulsion polymerization systems, increasing the emulsifier concentration results in a greater number density of micelles and thus in a greater number of growing polymer chains.[55,67] Additionally, increasing the amount of initiator leads to a higher initiation rate. The observed trend in the reaction rates could be explained by these two factors.

The kinetic data revealed three periods of polymerization for all four reactions. Each of the reactions begun with an acceleration period, the length of which was somewhat dependent on both the initial monomer concentration and the feed ratio. As the reaction reached a

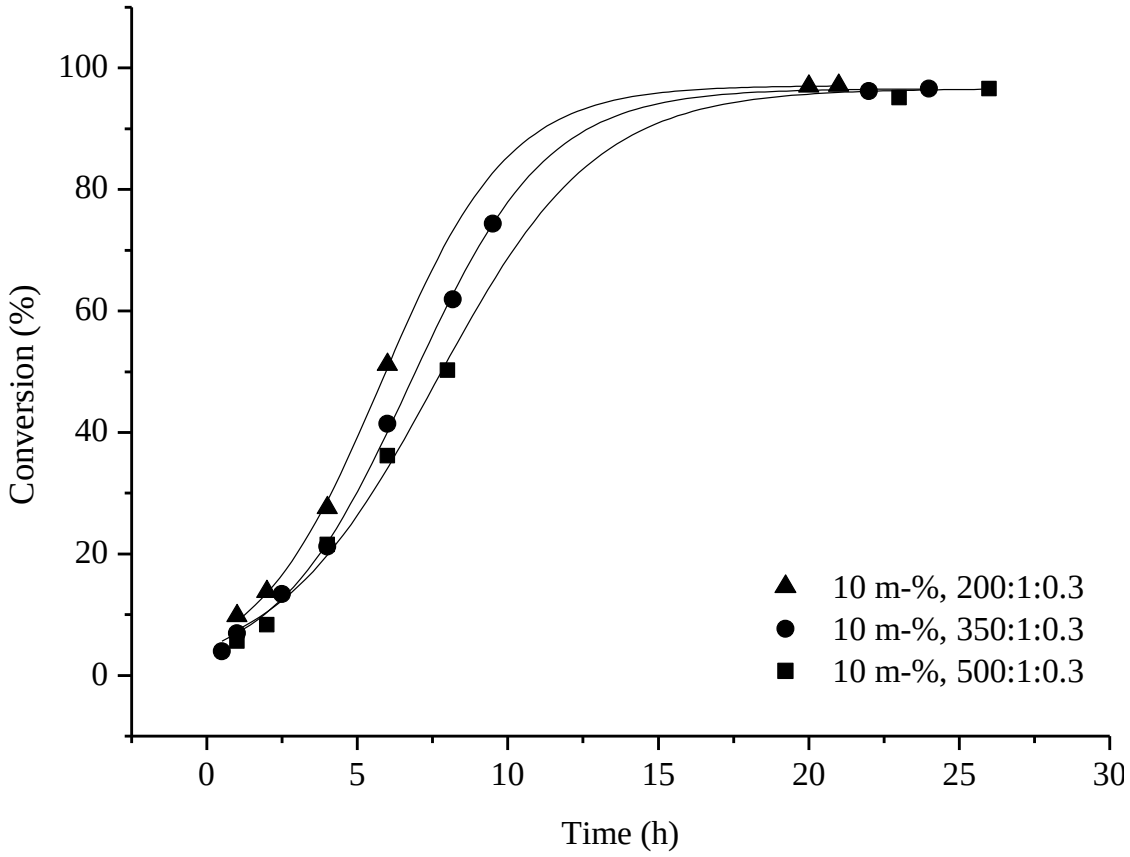

Figure 18 The effect of feed ratios on the reaction rate. NVCL was polymerized in the presence of $mPEG_{113}$-X using a 10 m-% initial monomer content. The three curves correspond to different $[M_0]$:[CTA]:[I] ratios. Conversion was determined by ^1H NMR analysis (2 drops of reaction mixture in 0.6 ml of D_2O).

20-30% conversion, a period of constant rate took place. High reaction rates allowed for the constant rate to be maintained until high conversions were reached. Conversely, low reaction rates promoted a faster transition to the deceleration phase. All reactions reached almost full conversion. However, for the 20 m-% reaction the reaction time was significantly shorter than for the rest.

14. Conclusions

A new PISA formulation was developed for producing PEG-*b*-PNVCL particles in water. The effects of reaction conditions were thoroughly studied, and the products were characterized using various techniques. The approach was shown to produce copolymer particles with well-defined properties which can be tuned by varying the reaction conditions. The particles can be physically crosslinked to make them insoluble in water at ambient temperatures. Furthermore, a simplified method for the modification of mPEG-OH into a xanthate-terminated mCTA was reported.

This work demonstrated the importance of the selection of stabilizer on the outcome of attempted PISA reactions. Successful stability of the particles was achieved using a PEG chain of 113 repeating units. The use of a shorter chain of 42 repeating units resulted in coagulum in the reaction flask. The relative volume fractions of the copolymer blocks have been shown to have a great effect on the result of several PISA reactions.[2] In addition to colloidal stability, the relationship can also affect the resulting morphology. As mPEG is commercially available at various molecular weights, the reaction could be further studied using stabilizers of different lengths. More importantly, further research is called for to determine the morphology of the particles. Development of the crosslinking procedure is needed, and other suitable crosslinkers should also be considered.

Based on the kinetic and chromatographic data, the polymerization reaction exhibited best qualities when performed at high concentrations. Such conditions resulted not only in high reaction rates and high yields, but also in lower dispersities of the products. The result suggested that the reaction could be even more successful at concentrations over 20 m-%. Thus, more research is needed to study the concentration dependence of the reaction in more depth. The kinetics resembled those of a typical emulsion polymerization process.[55] The reaction could be repeated using mPEG or a micelle-forming PEG derivative to better understand the role of mPEG-X in the reaction. Unwanted side reactions were avoided by carrying out the reaction in Tris buffer. However, the lipophilicity of Tris and the reactivity of its amine group makes it a non-ideal medium for the preparation of biocompatible materials.

This thesis reported one of the first PISA systems to exploit the temperature-sensitivity of the growing chain. Stimuli-responsive polymers can be expected to offer more exciting options for producing copolymer nano-objects. Moreover, the PISA concept was brought

closer to biomedical applications by using biocompatible polymers. The vast research already conducted on PEG and PVNCL make them ideal candidates in the search for new materials for applications such as drug delivery. As PISA has quickly become well recognized as an alternative method for designing polymer particles, the area of research will likely gain more popularity in the near future.

15. References

1. Rao, J. P. & Geckeler, K. E. Polymer nanoparticles: Preparation techniques and size-control parameters. *Prog. Polym. Sci.* **36,** 887–913 (2011).
2. Canning, S. L., Smith, G. N. & Armes, S. P. A Critical Appraisal of RAFT-Mediated Polymerization-Induced Self-Assembly. *Macromolecules* **49,** 1985–2001 (2016).
3. Tanner, P. *et al.* Polymeric Vesicles: From Drug Carriers to Nanoreactors and Artificial Organelles. *Acc. Chem. Res.* **44,** 1039–1049 (2011).
4. Blanazs, A. *et al.* Sterilizable Gels from Thermoresponsive Block Copolymer Worms. *J. Am. Chem. Soc.* **134,** 9741–9748 (2012).
5. Derry, M. J., Fielding, L. A. & Armes, S. P. Industrially-relevant polymerization-induced self-assembly formulations in non-polar solvents: RAFT dispersion polymerization of benzyl methacrylate. *Polym. Chem.* **6,** 3054–3062 (2015).
6. Ladmiral, V., Semsarilar, M., Canton, I. & Armes, S. P. Polymerization-Induced Self-Assembly of Galactose-Functionalized Biocompatible Diblock Copolymers for Intracellular Delivery. *J. Am. Chem. Soc.* **135,** 13574–13581 (2013).
7. Thompson, K. L. *et al.* Vermicious thermo-responsive Pickering emulsifiers. *Chem. Sci.* **6,** 4207–4214 (2015).
8. Figg, C. A. *et al.* Polymerization-induced thermal self-assembly (PITSA). *Chem. Sci.* **6,** 1230–1236 (2015).
9. Mai, Y. & Eisenberg, A. Self-assembly of block copolymers. *Chem. Soc. Rev.* **41,** 5969–5985 (2012).
10. Vihola, H., Laukkanen, A., Tenhu, H. & Hirvonen, J. Drug release characteristics of physically cross-linked thermosensitive poly(N-vinylcaprolactam) hydrogel particles. *J. Pharm. Sci.* **97,** 4783–4793 (2008).
11. Bader, H., Ringsdorf, H. & Schmidt, B. Watersoluble polymers in medicine. *Angew. Makromol. Chem.* **123,** 457–485 (1984).
12. Antonietti, M., Wenz, E., Bronstein, L. & Seregina, M. Synthesis and characterization of noble metal colloids in block copolymer micelles. *Adv. Mater.* **7,** 1000–1005 (1995).
13. Riess, G. Micellization of block copolymers. *Prog. Polym. Sci.* **28,** 1107–1170 (2003).
14. Menger, F. M. & Angelova, M. I. Giant Vesicles: Imitating the Cytological Processes of Cell Membranes. *Acc. Chem. Res.* **31,** 789–797 (1998).

15. Shum, H. C., Kim, J.-W. & Weitz, D. A. Microfluidic Fabrication of Monodisperse Biocompatible and Biodegradable Polymersomes with Controlled Permeability. *J. Am. Chem. Soc.* **130,** 9543–9549 (2008).
16. Gao, Z., Varshney, S. K., Wong, S. & Eisenberg, A. Block Copolymer 'Crew-Cut' Micelles in Water. *Macromolecules* **27,** 7923–7927 (1994).
17. Geng, Y. & Discher, D. E. Hydrolytic Degradation of Poly(ethylene oxide)-block-Polycaprolactone Worm Micelles. *J. Am. Chem. Soc.* **127,** 12780–12781 (2005).
18. Rodríguez-Hernández, J. & Lecommandoux, S. Reversible Inside−Out Micellization of pH-responsive and Water-Soluble Vesicles Based on Polypeptide Diblock Copolymers. *J. Am. Chem. Soc.* **127,** 2026–2027 (2005).
19. Zhang, L. & Eisenberg, A. Multiple Morphologies and Characteristics of "Crew-Cut" Micelle-like Aggregates of Polystyrene-b-poly(acrylic acid) Diblock Copolymers in Aqueous Solutions. *J. Am. Chem. Soc.* **118,** 3168–3181 (1996).
20. Groison, E. *et al.* Well-Defined Amphiphilic Block Copolymer Nanoobjects via Nitroxide-Mediated Emulsion Polymerization. *ACS Macro Lett.* **1,** 47–51 (2012).
21. Kim, K. H., Kim, J. & Jo, W. H. Preparation of hydrogel nanoparticles by atom transfer radical polymerization of N-isopropylacrylamide in aqueous media using PEG macro-initiator. *Polymer* **46,** 2836–2840 (2005).
22. Wan, W.-M. & Pan, C.-Y. Formation of Polymeric Yolk/Shell Nanomaterial by Polymerization-Induced Self-Assembly and Reorganization. *Macromolecules* **43,** 2672–2675 (2010).
23. Blanazs, A., Madsen, J., Battaglia, G., Ryan, A. J. & Armes, S. P. Mechanistic Insights for Block Copolymer Morphologies: How Do Worms Form Vesicles? *J. Am. Chem. Soc.* **133,** 16581–16587 (2011).
24. Fielding, L. A., Lane, J. A., Derry, M. J., Mykhaylyk, O. O. & Armes, S. P. Thermo-responsive Diblock Copolymer Worm Gels in Non-polar Solvents. *J. Am. Chem. Soc.* **136,** 5790–5798 (2014).
25. Lovett, J. R., Warren, N. J., Ratcliffe, L. P. D., Kocik, M. K. & Armes, S. P. pH-Responsive Non-Ionic Diblock Copolymers: Ionization of Carboxylic Acid End-Groups Induces an Order–Order Morphological Transition. *Angew. Chem. Int. Ed.* **54,** 1279–1283 (2015).
26. Dong, S., Zhao, W., Lucien, F. P., Perrier, S. & Zetterlund, P. B. Polymerization induced self-assembly: tuning of nano-object morphology by use of CO2. *Polym. Chem.* **6,** 2249–2254 (2015).

27. Aseyev, V., Tenhu, H. & Winnik, F. M. Non-ionic Thermoresponsive Polymers in Water. in *Self Organized Nanostructures of Amphiphilic Block Copolymers II* 29–89 (Springer, Berlin, Heidelberg, 2010). doi:10.1007/12_2010_57

28. Seuring, J. & Agarwal, S. Polymers with Upper Critical Solution Temperature in Aqueous Solution. *Macromol. Rapid Commun.* **33,** 1898–1920 (2012).

29. Sugihara, S., Armes, S. P., Blanazs, A. & Lewis, A. L. Non-spherical morphologies from cross-linked biomimetic diblock copolymers using RAFT aqueous dispersion polymerization. *Soft Matter* **7,** 10787–10793 (2011).

30. Chambon, P., Blanazs, A., Battaglia, G. & Armes, S. P. How Does Cross-Linking Affect the Stability of Block Copolymer Vesicles in the Presence of Surfactant? *Langmuir* **28,** 1196–1205 (2012).

31. Cortez-Lemus, N. A. & Licea-Claverie, A. Poly(N-vinylcaprolactam), a comprehensive review on a thermoresponsive polymer becoming popular. *Prog. Polym. Sci.* **53,** 1–51 (2016).

32. Shostakovsky, M. F., Sidelkovskaya, F. P. & Zelenskaya, M. G. Synthesis and transformations of vinylcaprolactam Part 1. Polymerization in presence of hydrogen peroxide. *Bull. Acad. Sci. USSR Div. Chem. Sci.* **1,** 633–636 (1952).

33. Solomon, O. F., Corciovei, M., Ciută, I. & Boghină, C. Properties of solutions of poly-N-vinylcaprolactam. *J. Appl. Polym. Sci.* **12,** 1835–1842 (1968).

34. Lozinsky, V. I. *et al.* Synthesis of N-vinylcaprolactam polymers in water-containing media. *Polymer* **41,** 6507–6518 (2000).

35. Beija, M., Marty, J.-D. & Destarac, M. Thermoresponsive poly(N-vinyl caprolactam)-coated gold nanoparticles: sharp reversible response and easy tunability. *Chem. Commun.* **47,** 2826–2828 (2011).

36. Medeiros, S. F., Barboza, J. C. S., Ré, M. I., Giudici, R. & Santos, A. M. Solution polymerization of N-vinylcaprolactam in 1,4-dioxane. Kinetic dependence on temperature, monomer, and initiator concentrations. *J. Appl. Polym. Sci.* **118,** 229–240 (2010).

37. Zhang, L., Liang, Y. & Meng, L. Thermo-sensitive amphiphilic poly(N-vinylcaprolactam) copolymers: synthesis and solution properties. *Polym. Adv. Technol.* **21,** 720–725 (2010).

38. Eisele, M. & Burchard, W. Hydrophobic water-soluble polymers, 1. Dilute solution properties of poly(1-vinyl-2-piperidone) and poly(N-vinylcaprolactam). *Makromol. Chem.* **191,** 169–184 (1990).

39. Meeussen, F. *et al.* Phase behaviour of poly(N-vinyl caprolactam) in water. *Polymer* **41,** 8597–8602 (2000).

40. Kermagoret, A. *et al.* One-pot controlled synthesis of double thermoresponsive N-vinylcaprolactam-based copolymers with tunable LCSTs. *Polym. Chem.* **4,** 2575–2583 (2013).

41. Okhapkin, I. M., Nasimova, I. R., Makhaeva, E. E. & Khokhlov, A. R. Effect of Complexation of Monomer Units on pH- and Temperature-Sensitive Properties of Poly(N-vinylcaprolactam-co-methacrylic acid). *Macromolecules* **36,** 8130–8138 (2003).

42. Liang, X. *et al.* Synthesis and self-assembly of thermosensitive double-hydrophilic poly(N-vinylcaprolactam)-b-poly(N-vinyl-2-pyrrolidone) diblock copolymers. *J. Polym. Sci. Part Polym. Chem.* **52,** 2725–2737 (2014).

43. Liu, J. *et al.* Gold nanorods coated with a thermo-responsive poly(ethylene glycol)-b-poly(N-vinylcaprolactam) corona as drug delivery systems for remotely near infrared-triggered release. *Polym. Chem.* **5,** 799–813 (2013).

44. Sofia, S. J. & Merrill, E. W. Protein Adsorption on Poly(ethylene oxide)-Grafted Silicon Surfaces. in *Poly(ethylene glycol)* **680,** 342–360 (American Chemical Society, 1997).

45. Vihola, H., Laukkanen, A., Valtola, L., Tenhu, H. & Hirvonen, J. Cytotoxicity of thermosensitive polymers poly(N-isopropylacrylamide), poly(N-vinylcaprolactam) and amphiphilically modified poly(N-vinylcaprolactam). *Biomaterials* **26,** 3055–3064 (2005).

46. Prabaharan, M., Grailer, J. J., Steeber, D. A. & Gong, S. Stimuli-Responsive Chitosan-graft-Poly(N-vinylcaprolactam) as a Promising Material for Controlled Hydrophobic Drug Delivery. *Macromol. Biosci.* **8,** 843–851 (2008).

47. Prabaharan, M., Grailer, J. J., Steeber, D. A. & Gong, S. Thermosensitive Micelles Based on Folate-Conjugated Poly(N-vinylcaprolactam)-block-Poly(ethylene glycol) for Tumor-Targeted Drug Delivery. *Macromol. Biosci.* **9,** 744–753 (2009).

48. Imaz, A. & Forcada, J. N-vinylcaprolactam-based microgels for biomedical applications. *J. Polym. Sci. Part Polym. Chem.* **48,** 1173–1181 (2010).

49. Sun, X.-Z., Wang, X., Wu, J.-Z. & Li, S.-D. Development of thermosensitive microgel-loaded cotton fabric for controlled drug release. *Appl. Surf. Sci.* **403,** 509–518 (2017).

50. Medeiros, S. F., Lopes, M. V., Rossi-Bergmann, B., Ré, M. I. & Santos, A. M. Synthesis and characterization of poly(N-vinylcaprolactam)-based spray-dried microparticles exhibiting temperature and pH-sensitive properties for controlled release of ketoprofen. *Drug Dev. Ind. Pharm.* **43,** 1519–1529 (2017).

51. Shah, S., Pal, A., Gude, R. & Devi, S. Synthesis and characterization of thermo-responsive copolymeric nanoparticles of poly(methyl methacrylate-co-N-vinylcaprolactam). *Eur. Polym. J.* **46,** 958–967 (2010).

52. Markvicheva, E. A. *et al.* A novel technique for entrapment of hybridoma cells in synthetic thermally reversible polymers. *Biotechnol. Tech.* **5,** 223–226 (1991).

53. Chiefari, J. *et al.* Living Free-Radical Polymerization by Reversible Addition−Fragmentation Chain Transfer: The RAFT Process. *Macromolecules* **31,** 5559–5562 (1998).

54. Perrier, S. & Takolpuckdee, P. Macromolecular design via reversible addition–fragmentation chain transfer (RAFT)/xanthates (MADIX) polymerization. *J. Polym. Sci. Part Polym. Chem.* **43,** 5347–5393 (2005).

55. Mandal, B. M. *Fundamentals of Polymerization*. (World Scientific, 2013).

56. Cacioli, P., Hawthorne, D. G., Laslett, R. L., Rizzardo, E. & Solomon, D. H. Copolymerization of ω-Unsaturated Oligo(Methyl Methacrylate): New Macromonomers. *J. Macromol. Sci. Part - Chem.* **23,** 839–852 (1986).

57. Delduc, P., Tailhan, C. & Zard, S. Z. A convenient source of alkyl and acyl radicals. *J. Chem. Soc. Chem. Commun.* **0,** 308–310 (1988).

58. Mayadunne, R. T. A. *et al.* Living Radical Polymerization with Reversible Addition−Fragmentation Chain Transfer (RAFT Polymerization) Using Dithiocarbamates as Chain Transfer Agents. *Macromolecules* **32,** 6977–6980 (1999).

59. Barner-Kowollik, C. *Handbook of RAFT Polymerization*. (John Wiley & Sons, 2008).

60. Wan, D., Zhou, Q., Pu, H. & Yang, G. Controlled radical polymerization of N-vinylcaprolactam mediated by xanthate or dithiocarbamate. *J. Polym. Sci. Part Polym. Chem.* **46,** 3756–3765 (2008).

61. Nieuwenhove, I. V. *et al.* RAFT/MADIX polymerization of N-vinylcaprolactam in water–ethanol solvent mixtures. *Polym. Chem.* **8,** 2433–2437 (2017).

62. Donovan, M. S., Lowe, A. B., Sanford, T. A. & McCormick, C. L. Sulfobetaine-containing diblock and triblock copolymers via reversible addition-fragmentation chain transfer polymerization in aqueous media. *J. Polym. Sci. Part Polym. Chem.* **41,** 1262–1281 (2003).

63. Mayadunne, R. T. A. *et al.* Living Polymers by the Use of Trithiocarbonates as Reversible Addition−Fragmentation Chain Transfer (RAFT) Agents: ABA Triblock Copolymers by Radical Polymerization in Two Steps. *Macromolecules* **33,** 243–245 (2000).

64. Hong, C.-Y., You, Y.-Z. & Pan, C.-Y. Synthesis and characterization of well-defined diblock and triblock copolymers of poly(N-isopropylacrylamide) and poly(ethylene oxide). *J. Polym. Sci. Part Polym. Chem.* **42,** 4873–4881 (2004).

65. Shi, L., Chapman, T. M. & Beckman, E. J. Poly(ethylene glycol)-block-poly(N-vinylformamide) Copolymers Synthesized by the RAFT Methodology. *Macromolecules* **36,** 2563–2567 (2003).

66. Okubo, M. *Polymer Particles*. (Springer Science & Business Media, 2005).

67. Rieger, J. *et al.* Amphiphilic Poly(ethylene oxide) Macromolecular RAFT Agent as a Stabilizer and Control Agent in ab Initio Batch Emulsion Polymerization. *Macromolecules* **41,** 4065–4068 (2008).

68. Etchenausia, L., Khoukh, A., Lejeune, E. D. & Save, M. RAFT/MADIX emulsion copolymerization of vinyl acetate and N-vinylcaprolactam: towards waterborne physically crosslinked thermoresponsive particles. *Polym. Chem.* **8,** 2244–2256 (2017).

69. Harkins, W. D. A General Theory of the Mechanism of Emulsion Polymerization1. *J. Am. Chem. Soc.* **69,** 1428–1444 (1947).

70. Smith, W. V. & Ewart, R. H. Kinetics of Emulsion Polymerization. *J. Chem. Phys.* **16,** 592–599 (1948).

71. Charleux, B., Delaittre, G., Rieger, J. & D'Agosto, F. Polymerization-Induced Self-Assembly: From Soluble Macromolecules to Block Copolymer Nano-Objects in One Step. *Macromolecules* **45,** 6753–6765 (2012).

72. Manguian, M., Save, M. & Charleux, B. Batch Emulsion Polymerization of Styrene Stabilized by a Hydrophilic Macro-RAFT Agent. *Macromol. Rapid Commun.* **27,** 399–404 (2006).

73. Cunningham, V. J. *et al.* Poly(glycerol monomethacrylate)–Poly(benzyl methacrylate) Diblock Copolymer Nanoparticles via RAFT Emulsion Polymerization: Synthesis, Characterization, and Interfacial Activity. *Macromolecules* **47,** 5613–5623 (2014).

74. Nzudie, D. T., Dimonie, V. L., Sudol, E. D. & El-Aasser, M. S. Use of styrene-maleic anhydride copolymers (SMA resins) in emulsion copolymerization. *J. Appl. Polym. Sci.* **70,** 2729–2747 (1998).

75. Blanazs, A., Ryan, A. J. & Armes, S. P. Predictive Phase Diagrams for RAFT Aqueous Dispersion Polymerization: Effect of Block Copolymer Composition, Molecular Weight, and Copolymer Concentration. *Macromolecules* **45,** 5099–5107 (2012).

76. Perrier, S., Takolpuckdee, P. & Mars, C. A. Reversible Addition−Fragmentation Chain Transfer Polymerization: End Group Modification for Functionalized Polymers and Chain Transfer Agent Recovery. *Macromolecules* **38,** 2033–2036 (2005).
77. Dust, J. M., Fang, Z. H. & Harris, J. M. Proton NMR characterization of poly(ethylene glycols) and derivatives. *Macromolecules* **23,** 3742–3746 (1990).
78. Good, N. E. *et al.* Hydrogen Ion Buffers for Biological Research*. *Biochemistry (Mosc.)* **5,** 467–477 (1966).
79. Imaz, A., Miranda, J. I., Ramos, J. & Forcada, J. Evidences of a hydrolysis process in the synthesis of N-vinylcaprolactam-based microgels. *Eur. Polym. J.* **44,** 4002–4011 (2008).
80. Baicu, S. C. & Taylor, M. J. Acid–base buffering in organ preservation solutions as a function of temperature: new parameters for comparing buffer capacity and efficiency. *Cryobiology* **45,** 33–48 (2002).
81. Grady, J. K., Chasteen, N. D. & Harris, D. C. Radicals from 'Good's' buffers. *Anal. Biochem.* **173,** 111–115 (1988).
82. Canning, S. L., Cunningham, V. J., Ratcliffe, L. P. D. & Armes, S. P. Phenyl acrylate is a versatile monomer for the synthesis of acrylic diblock copolymer nano-objects via polymerization-induced self-assembly. *Polym. Chem.* **8,** 4811–4821 (2017).